

Implementation of Nonlinear Material Response in Scalable Earthquake Ground Motion Simulations

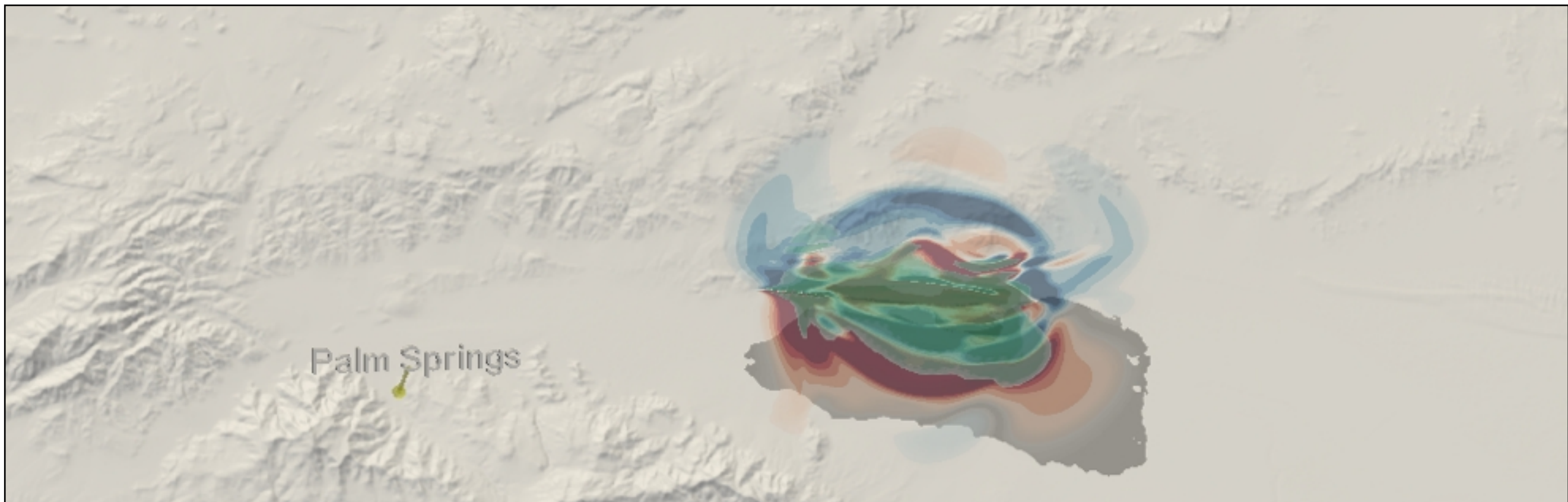
Roten, D.¹, Cui, Y., Olsen, K.B.², Day, S.M.² and Cui, Y.¹

1 San Diego Supercomputer Center

2 San Diego State University



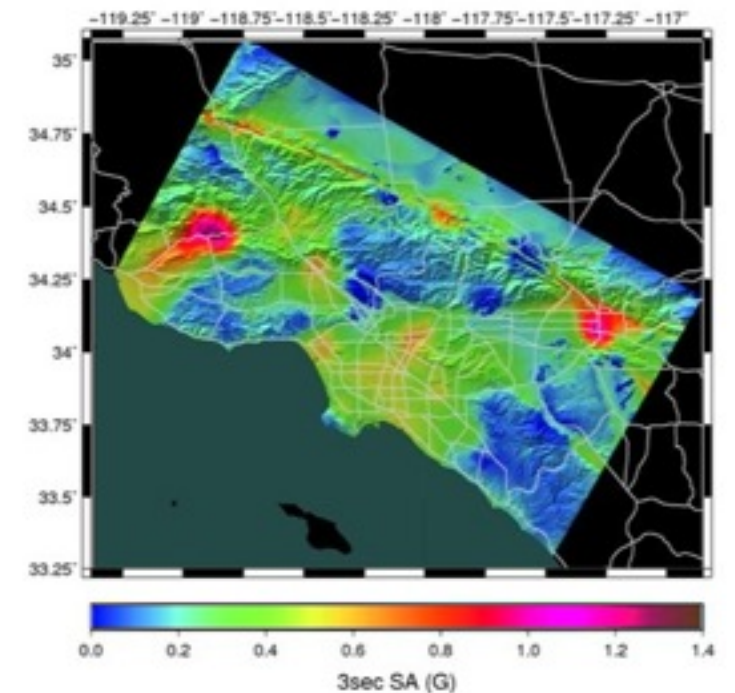
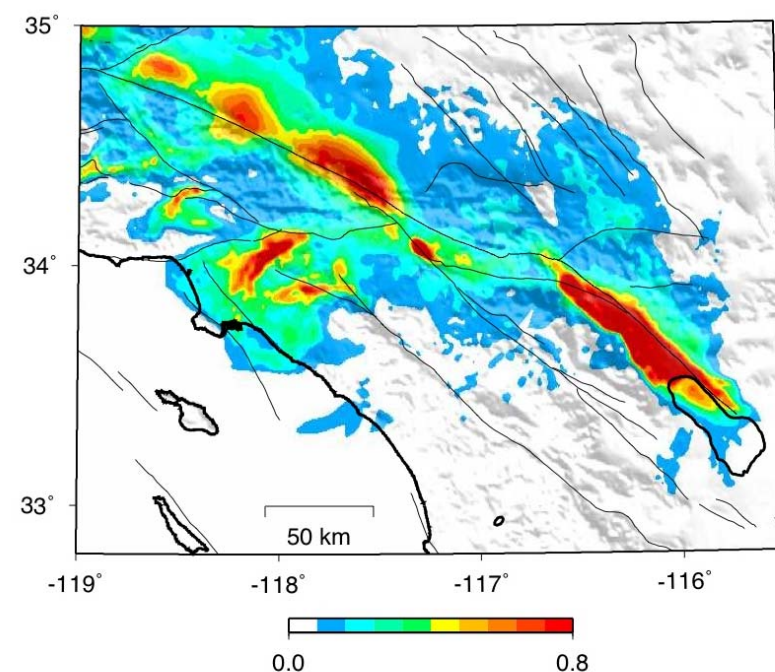
Symposium on HPC and Data-Intensive Applications in Earth Sciences: Challenges and Opportunities
Nov 13-14 2014, ICTP, Trieste, Italy



Background

3D wave propagation simulations of ground motions are already playing a role in assessment of hazard and risk:

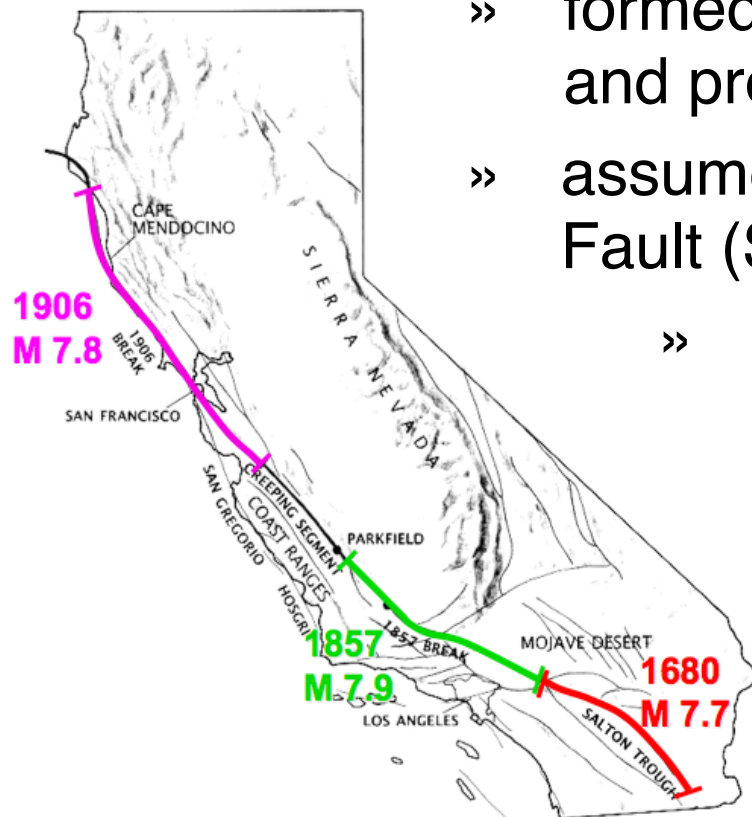
- » Prediction of ground motions from *scenario earthquakes* for planning of earthquake emergency response and public earthquake preparedness exercises
- » Physics-based seismic hazard assessment (e.g., Cybershake, Graves *et al.*, 2011)
- » Complement empirical ground motion prediction equations in regions of poor sampling



Background

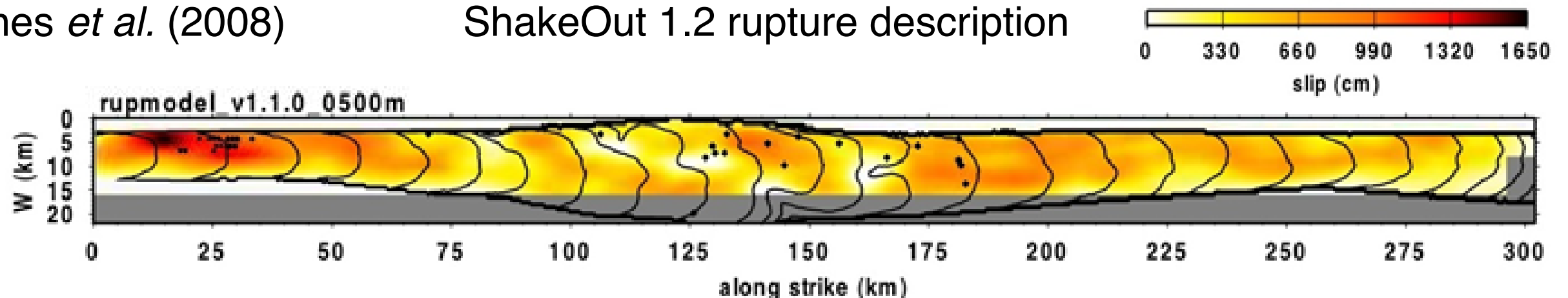
ShakeOut scenario simulations

- » formed the basis of the **ShakeOut** Earthquake emergency response and preparedness exercise (Jones *et al.*, 2008)
- » assumes a M 7.8 earthquake rupturing the southern San Andreas Fault (SAF) from Bombay Beach to Lake Hughes
 - » slip distribution and rupture times defined through **kinematic** source model (Graves *et al.*, 2008) based on expert opinion, empirical relationships and previous studies
 - » wave propagation modeled for **visco-elastic** medium by three different groups (Bielak *et al.*, 2010)



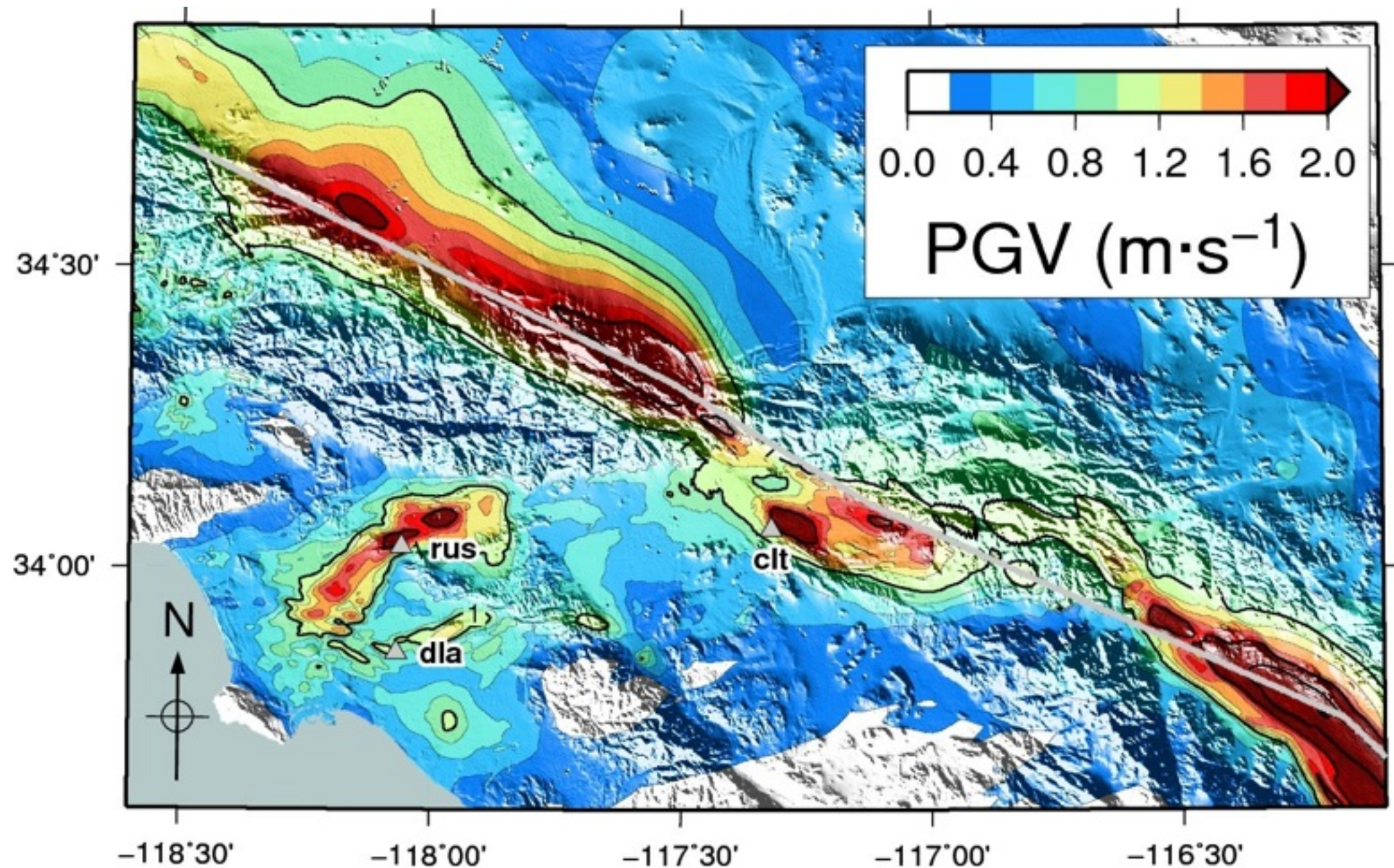
Jones *et al.* (2008)

ShakeOut 1.2 rupture description



Background

Sedimentary *waveguide* channeling surface waves from SAF into Los Angeles basin:
coupling of source directivity and basin response

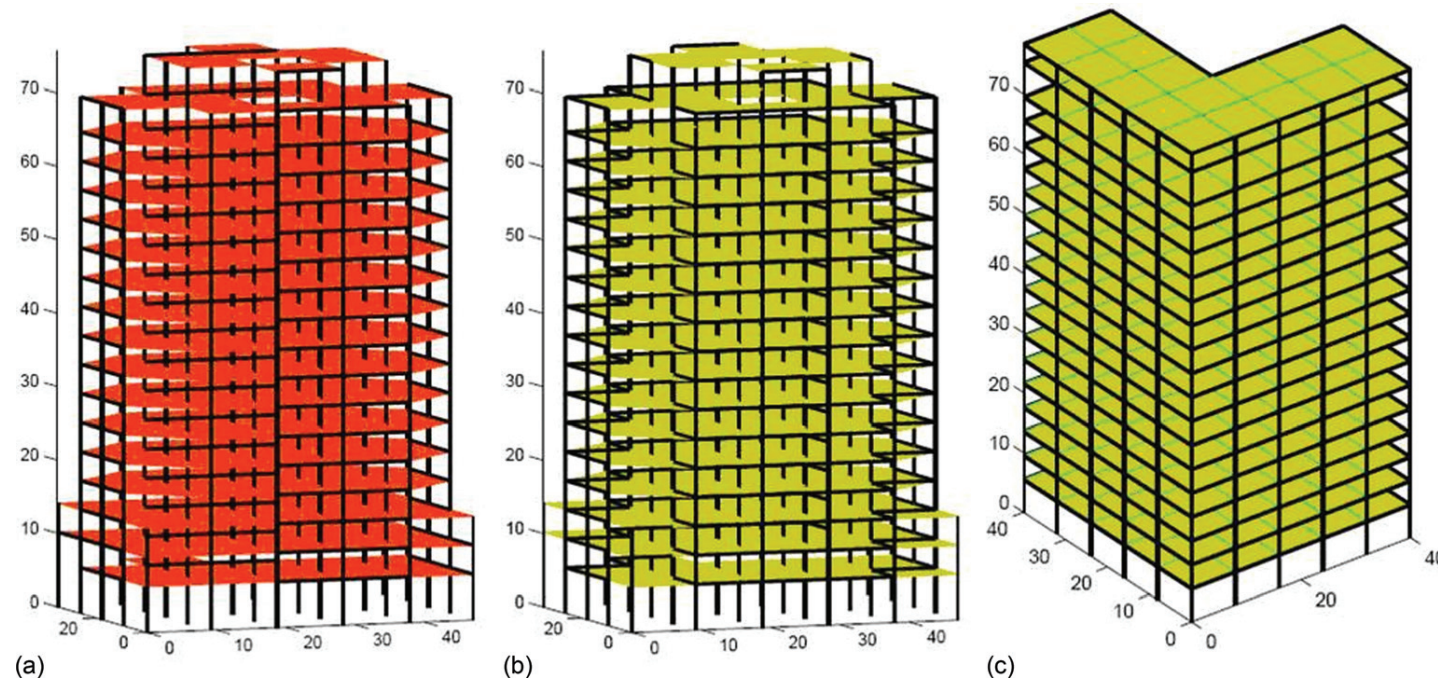


ShakeOut peak ground velocities for visco-elastic medium ($f_{\text{max}} = 0.5 \text{ Hz}$)

Background

Damage to pre-Northridge welded-steel moment-frame buildings (PNWSMF)

- » Brittle fractures in welded beam-to-column connections detected after 1994 Northridge earthquake
- » Response of PNWSMF buildings to ShakeOut ground motion analyzed through numerical modeling (Porter *et al.*, 2011)
- » Collapse of some (1-8) pre-1994 welded steel moment frame buildings deemed credible (Jones *et al.*, 2008)
- » 5 high-rise collapses assumed for ShakeOut scenario



Total fatalities	1779
Steel-Frame buildings	439
Other buildings	260
Fire	916
Transportation	164

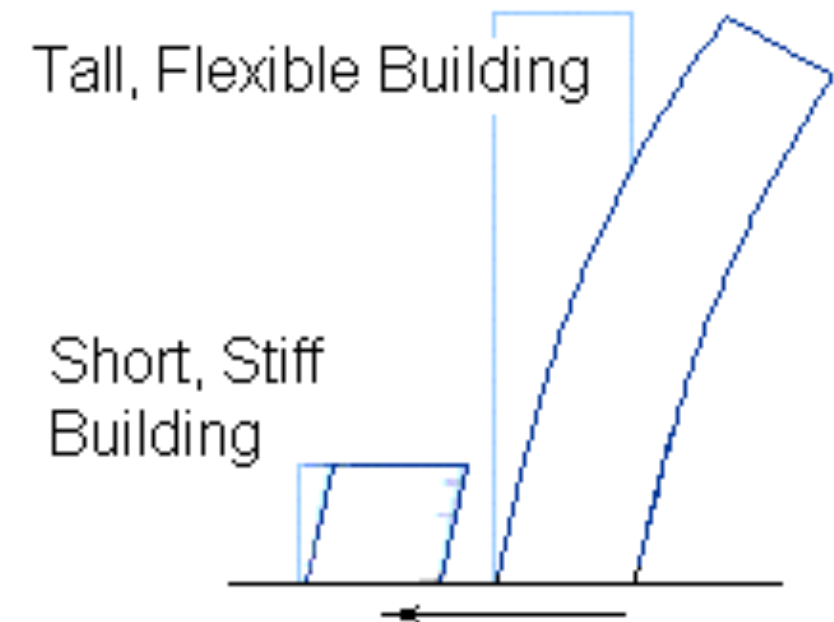
Natural Period of Buildings

$$f = \frac{1}{2\pi} \sqrt{\frac{K}{M}}$$

f : natural frequency (Hz)

K : the stiffness of the building with a specific mode

M : the mass of the building associated with the mode

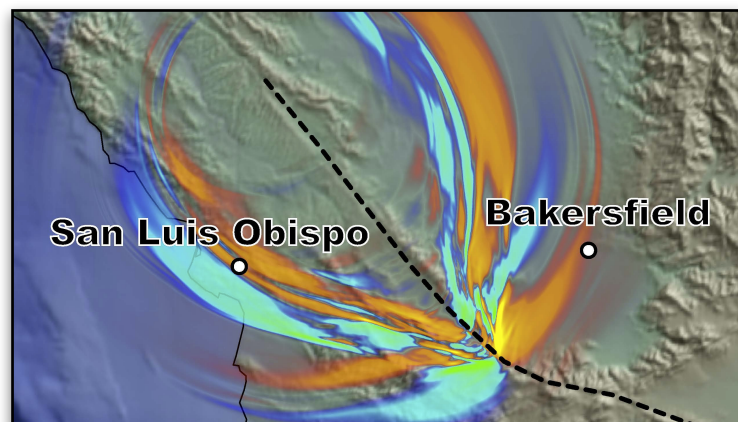


# Floors	Natural Period
2	0.2 s
5	0.5 s
10	1 s
20	2 s
30	3 s
50	5.0 s

2011 M_w 6.1 Christchurch Earthquake

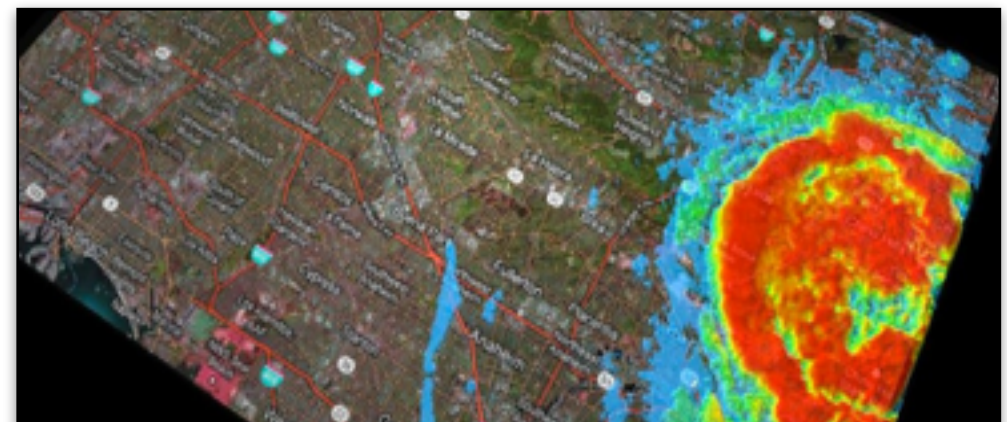
SCEC Milestone Simulations w/ AWP-ODC

Name	Year	System Number of Cores	Description	f
TeraShake 1.x	2004	SDSC Datastar 240 CPU cores	M_w (SAF)	0.5 Hz
Pacific NW Megathrust	2006	SDSC BlueGene 6,000 CPU cores	Long-Period ground motions for EQs in Cascadia subduction zone	0.5 Hz
ShakeOut 2.x	2008	TACC Ranger 32k CPU cores	M_w source description	1.0 Hz
M8	2010	ORNL Jaguar 223k CPU cores	M_w dynamic source	2.0 Hz
Chino Hills	2012	ORNL Titan 952 GPUs	2008 including small-scale heterogeneities	5.0 Hz
Rough faults	2014	ORNL Titan 16.6k GPUs	Statistical model of small scale heterogeneities, 20 m spacing	10.0 Hz



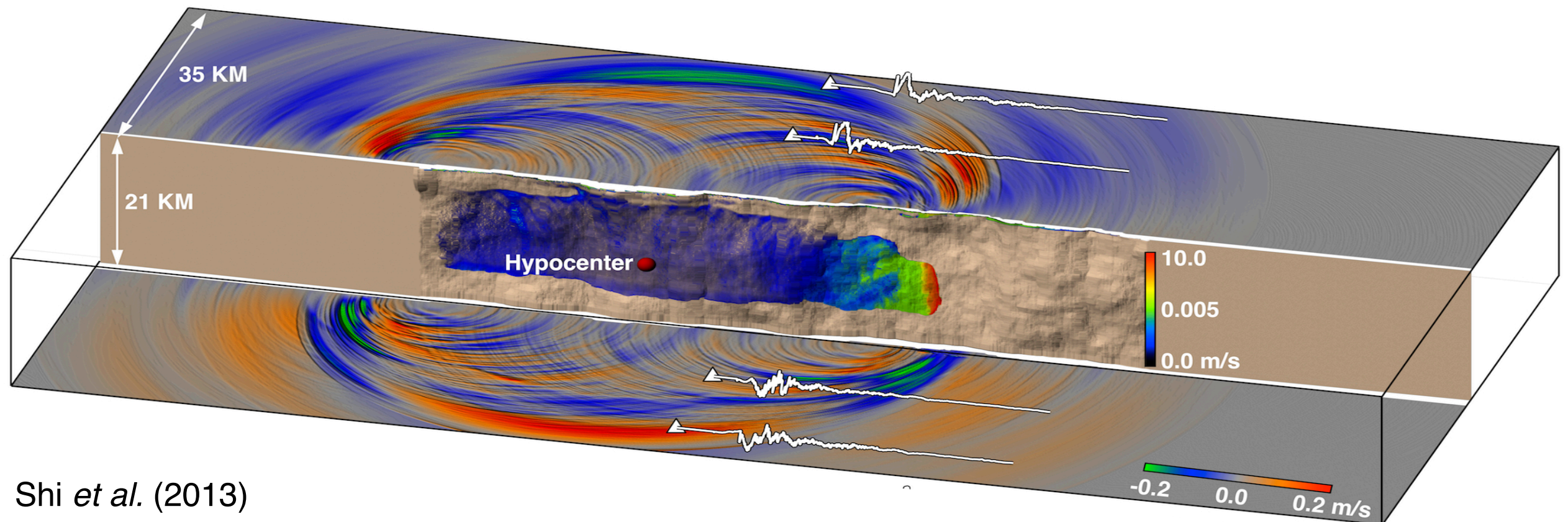
M8

Chino Hills



Challenges in HF Wave Propagation Simulations

- » Performance optimizations and the deployment of GPU-based supercomputers have pushed the *frequency limit* of deterministic ground motion prediction from ~ 1 to more than 5 Hz
- » In such high-frequency simulations, several aspects require special attention:
 - Generation of high frequencies at the source: dynamic rupture simulation of rough faults (Dunham *et al.*, 2011; Shi *et al.*, 2013) using SORD and AWP
 - Anelastic attenuation (frequency-dependent Q , e.g. Withers *et al.*, 2014)
 - Random heterogeneities in velocity structure (scattering, generation of seismic coda; e.g., Savran & Olsen, 2014)
 - *Nonlinear material response* in the fault damage zone (Andrews, 2005) and in near-surface sediments (e.g., Bonilla *et al.*, 2012)

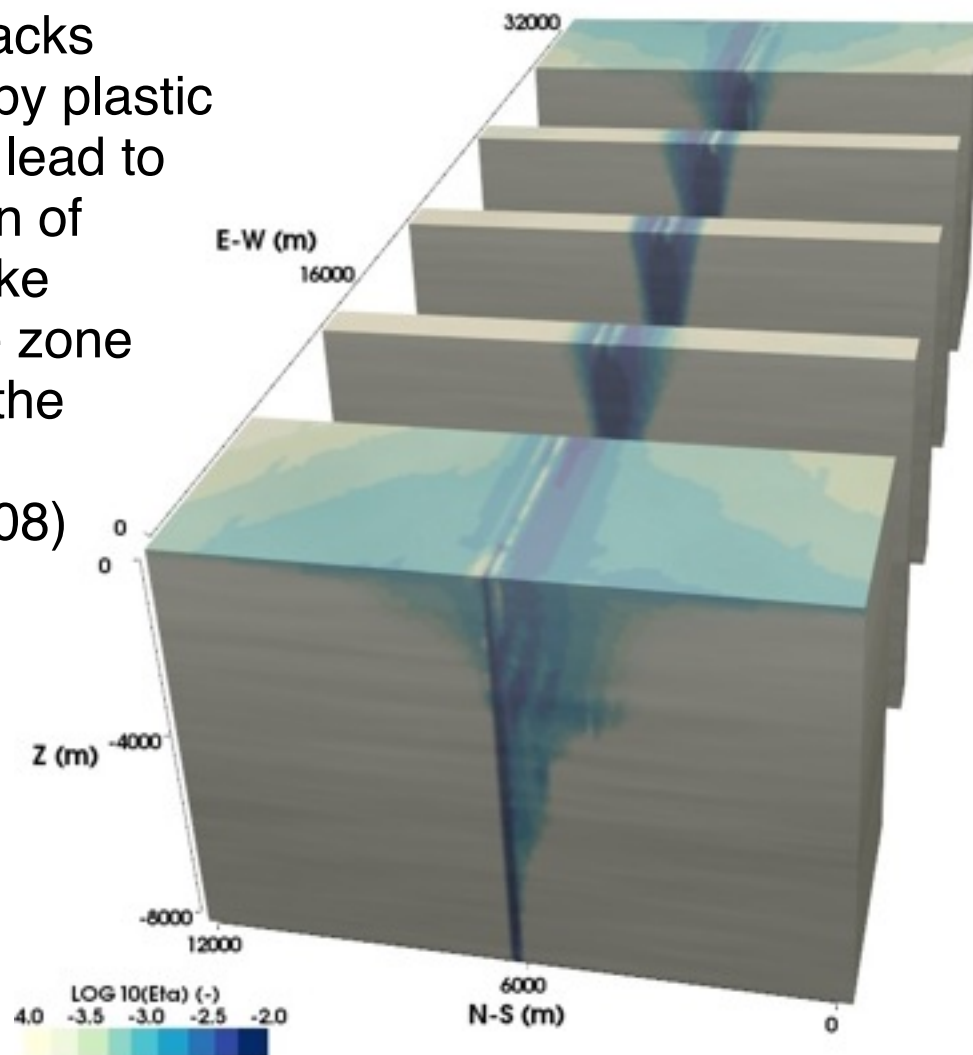


Shi *et al.* (2013)

Nonlinear Material Response

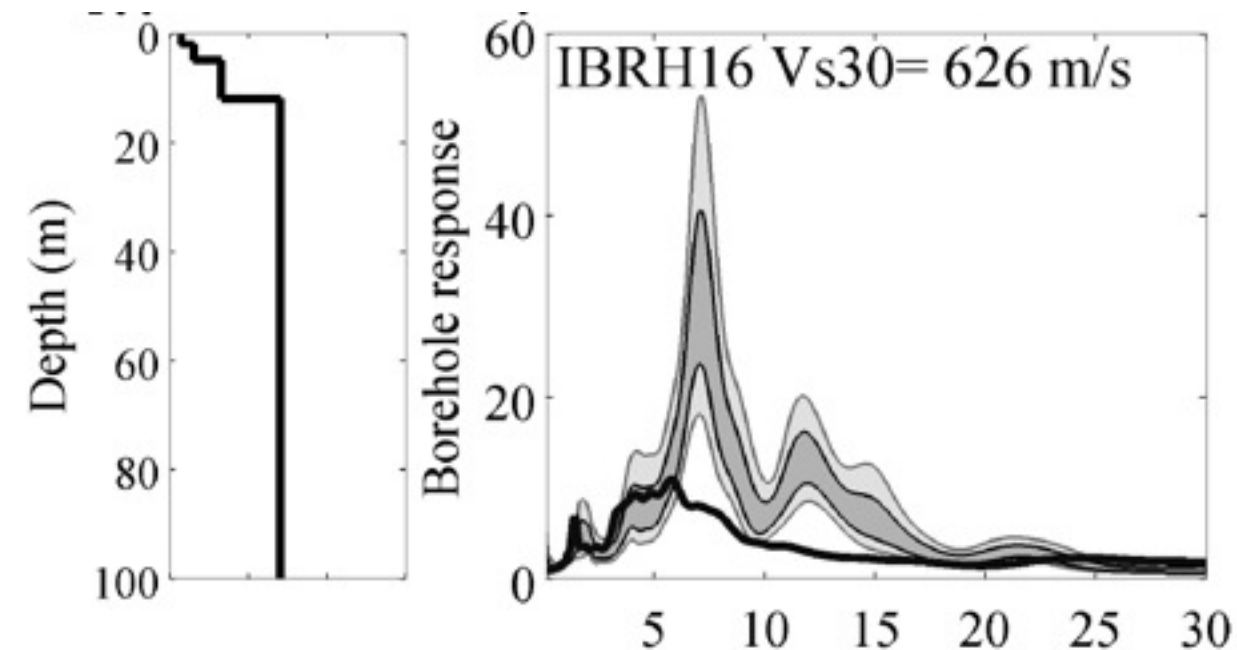
In the fault damage zone

- » Stresses at rupture front exceed strength of crustal rock, leading to permanent deformation near the fault
- » This effect may limit the peak velocity in ground motion caused by the rupture (Andrews *et al.*, 2007)
- » Microcracks formed by plastic yielding lead to evolution of flower-like damage zone around the fault (Ma, 2008)



In shallow sedimentary deposits

- » Stress-strain relationship in soils becomes nonlinear and hysteretic at large strains
- » Increased damping leads to a *reduction* in amplification (defined as ground motion on soil divided by bedrock ground motion) effects caused by soft soils



Bonilla *et al.* (2011)

AWP-ODC Finite Difference Code

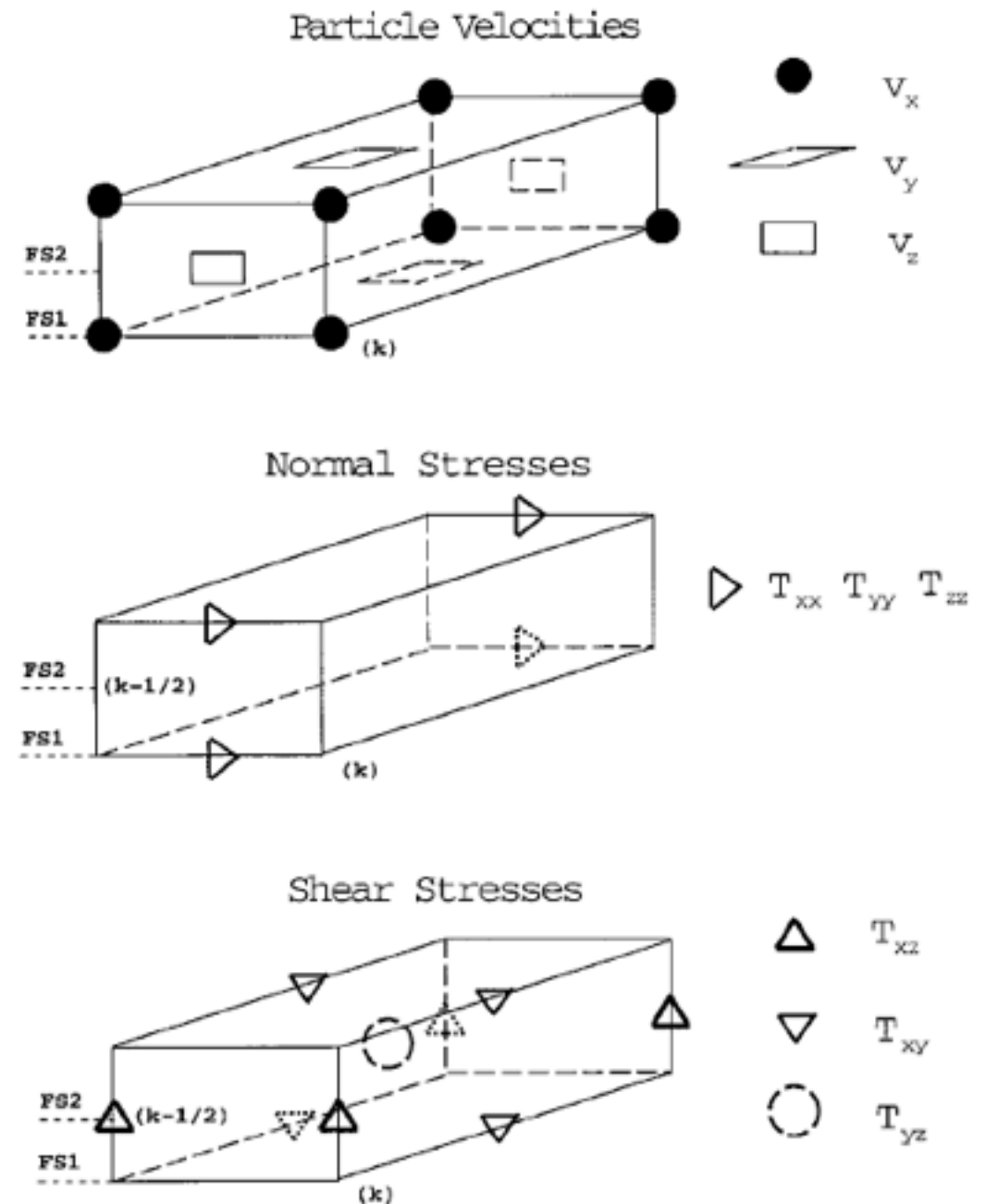
- » Started as a personal research code (Olsen, 1994)
- » 3D velocity-stress wave equations

$$\partial_t \mathbf{v} = \frac{1}{\rho} \nabla \cdot \sigma$$

$$\partial_t \sigma = \lambda (\nabla \cdot \mathbf{v}) I + \mu (\nabla \mathbf{v} + \nabla \mathbf{v}^T)$$

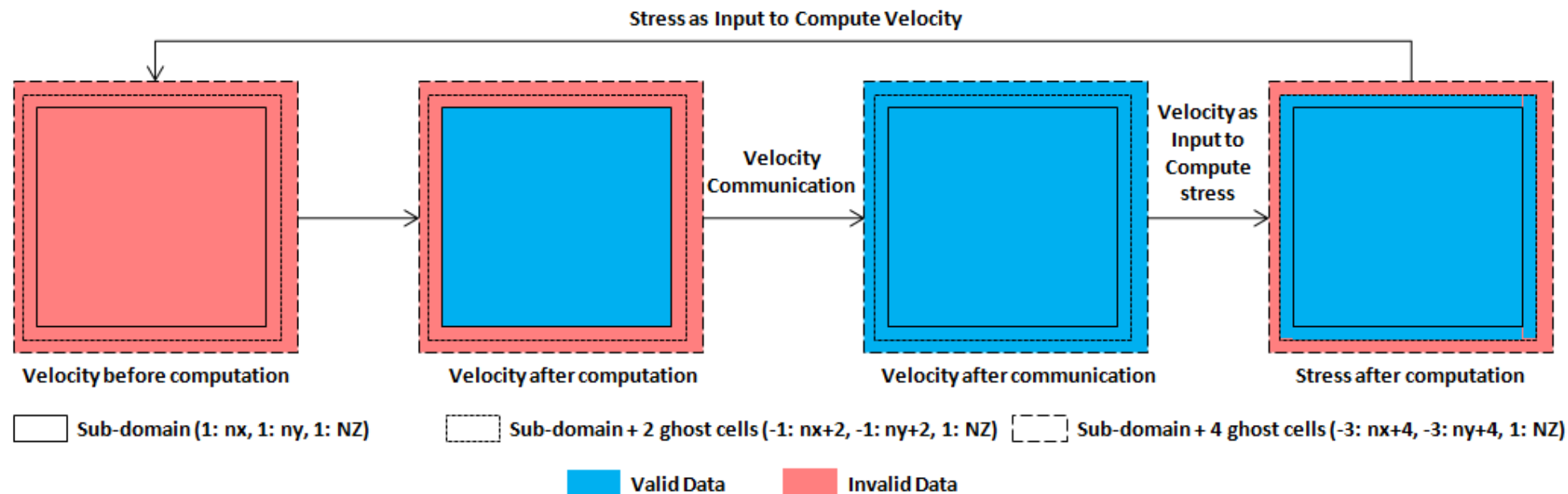
solved by *explicit staggered-grid 4th order* FD

- » Memory variable formulation of inelastic relaxation using coarse-grained representation (Day, 1998)
- » Dynamic rupture by the staggered-grid split-node (SGSN) method (Dalguer and Day 2007)
- » Absorbing boundary conditions by perfectly matched layers (PML) (Marcinkovich & Olsen, 2003) and Cerjan et al. (1985)
- » Parallelized using MPI and optimized for large-scale (>100k cores) simulations (Cui et al. 2010)



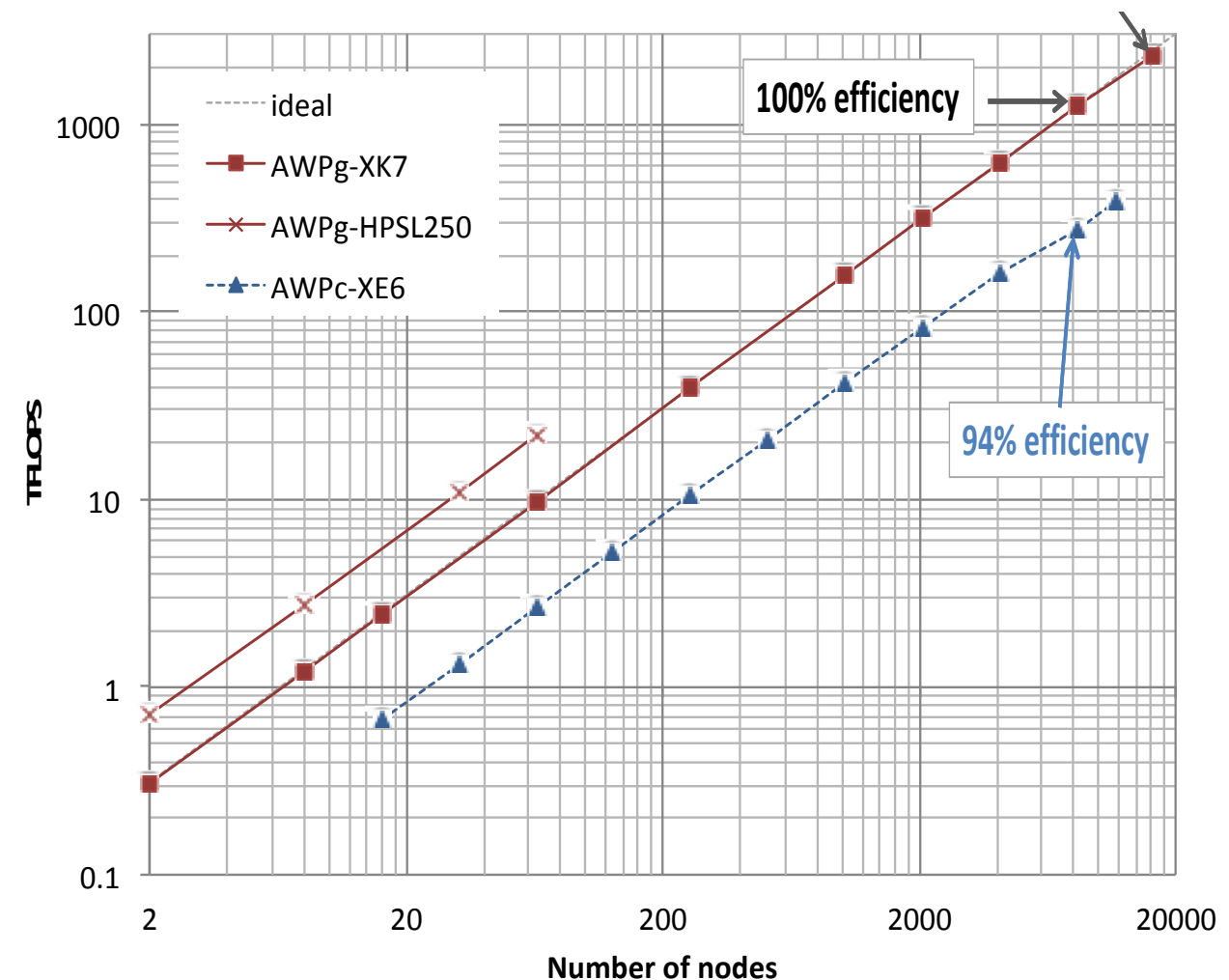
AWP-ODC GPU Finite Difference Code

(Zhou *et al.*, 2013)

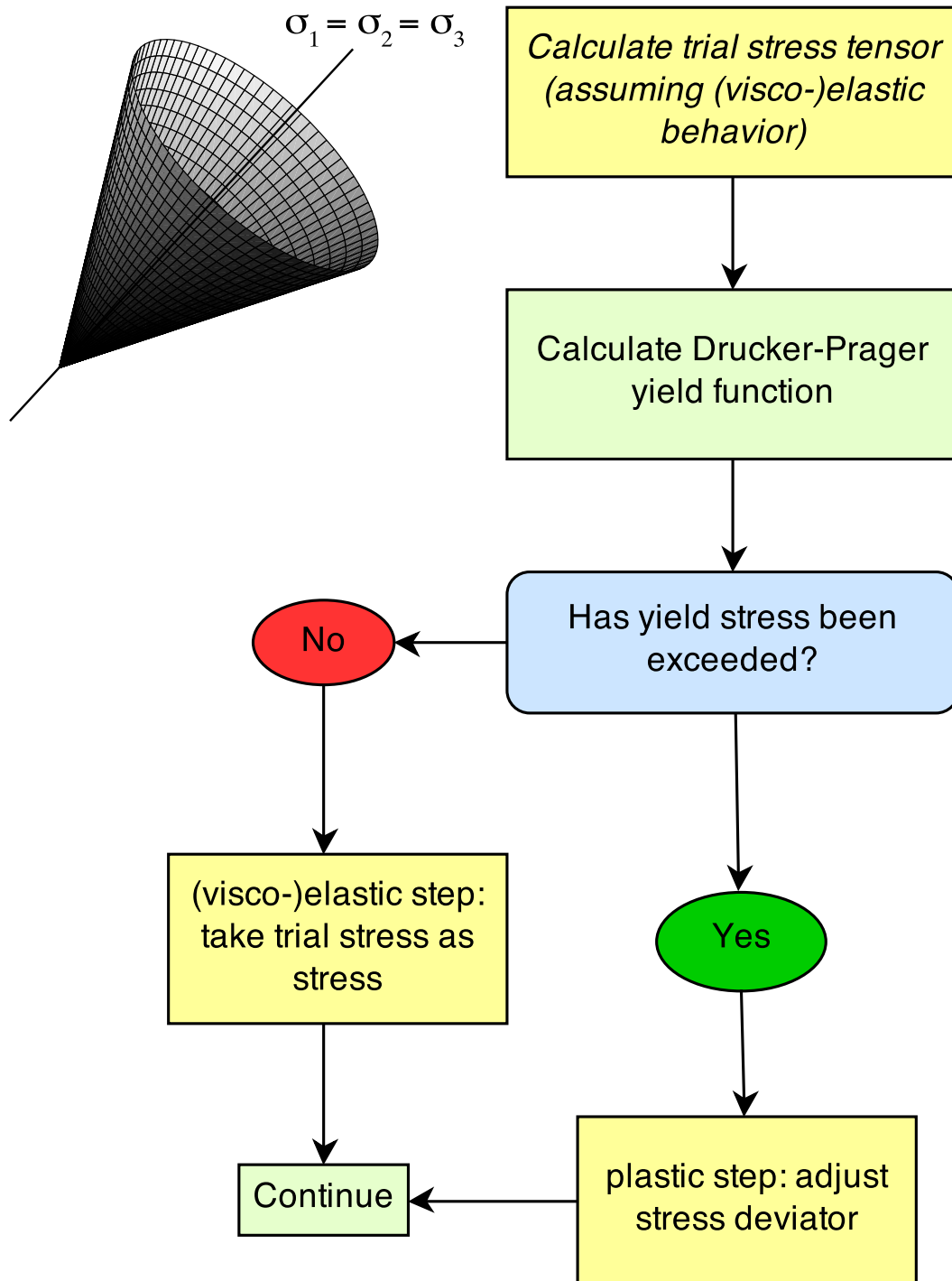


- » Hybrid MPI/CUDA version (w/o dynamic rupture and PMLs) developed by Zhou *et al.* (2013)
- » Communication reduction achieved by expanding ghost cells to 4 layers
- » Overlapping of communication and computation results in excellent scalability
- » Speedup of $\sim 3.8x$ on a node-to-node level between XK7 and XE6

(Cui *et al.*, 2013)



Return map algorithm in AWP-ODC FD code



Mean stress:

$$\tau_m = \frac{1}{3}(\sigma_{11} + \sigma_{22} + \sigma_{33}) = \frac{I_1}{3}$$

Stress deviator:

$$s_{ij} = \tau_{ij} - \tau_m \delta_{ij}$$

Second invariant of stress deviator:

$$J_2 = \frac{1}{2} \sum_{i,j} s_{ij} s_{ji}$$

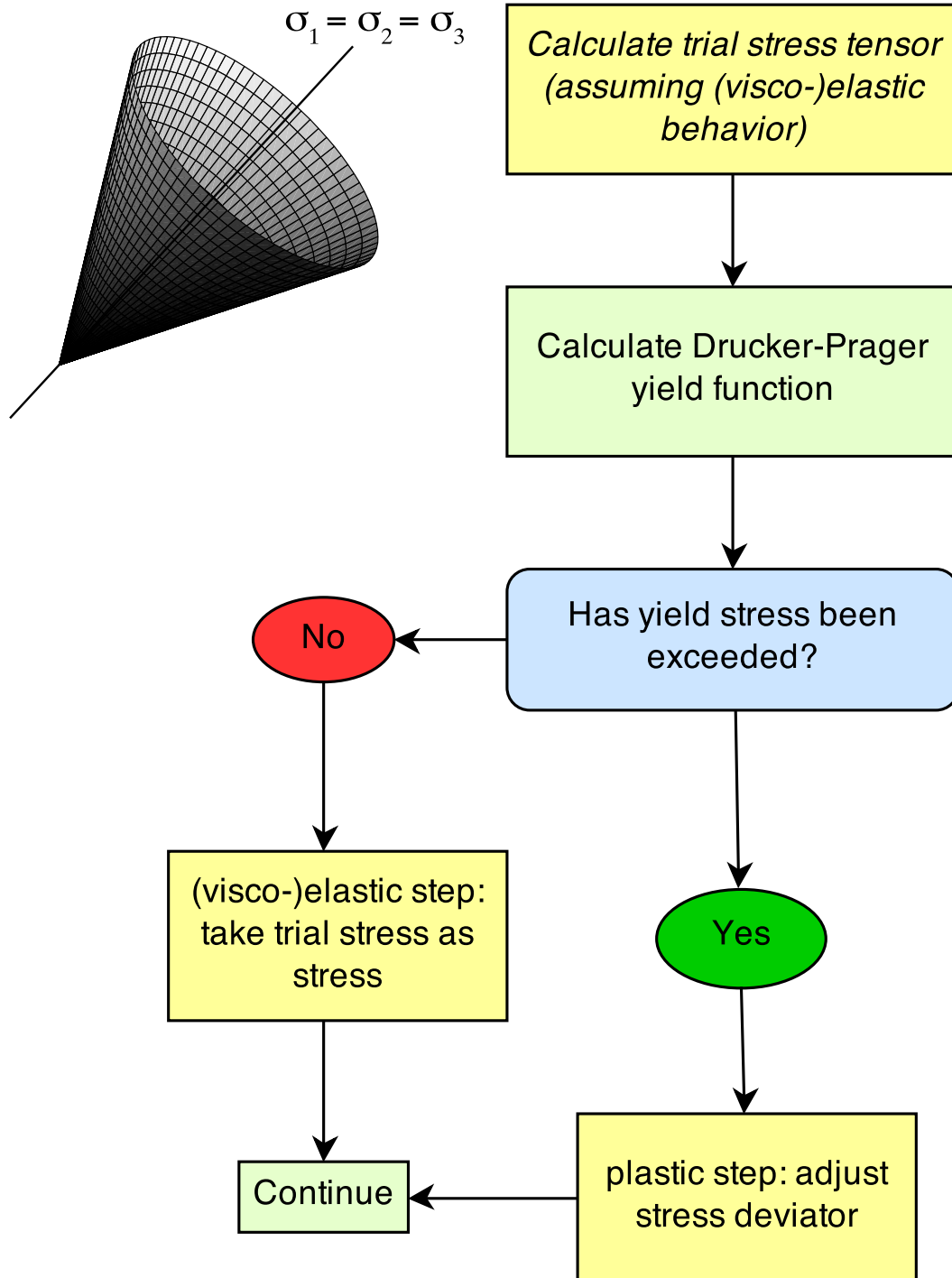
Drucker-Prager yield stress:

$$Y(\tau) = \max(0, c \cos \varphi - (\tau_m + P_f) \sin \varphi)$$

Drucker-Prager yield function:

$$F(\tau) = \sqrt{J_2(\tau)} - Y(\tau)$$

Return map algorithm in AWP-ODC FD code



Yield factor r :

$$r = \frac{Y(\tau^{\text{trial}})}{\sqrt{J_2(\tau^{\text{trial}})}}$$

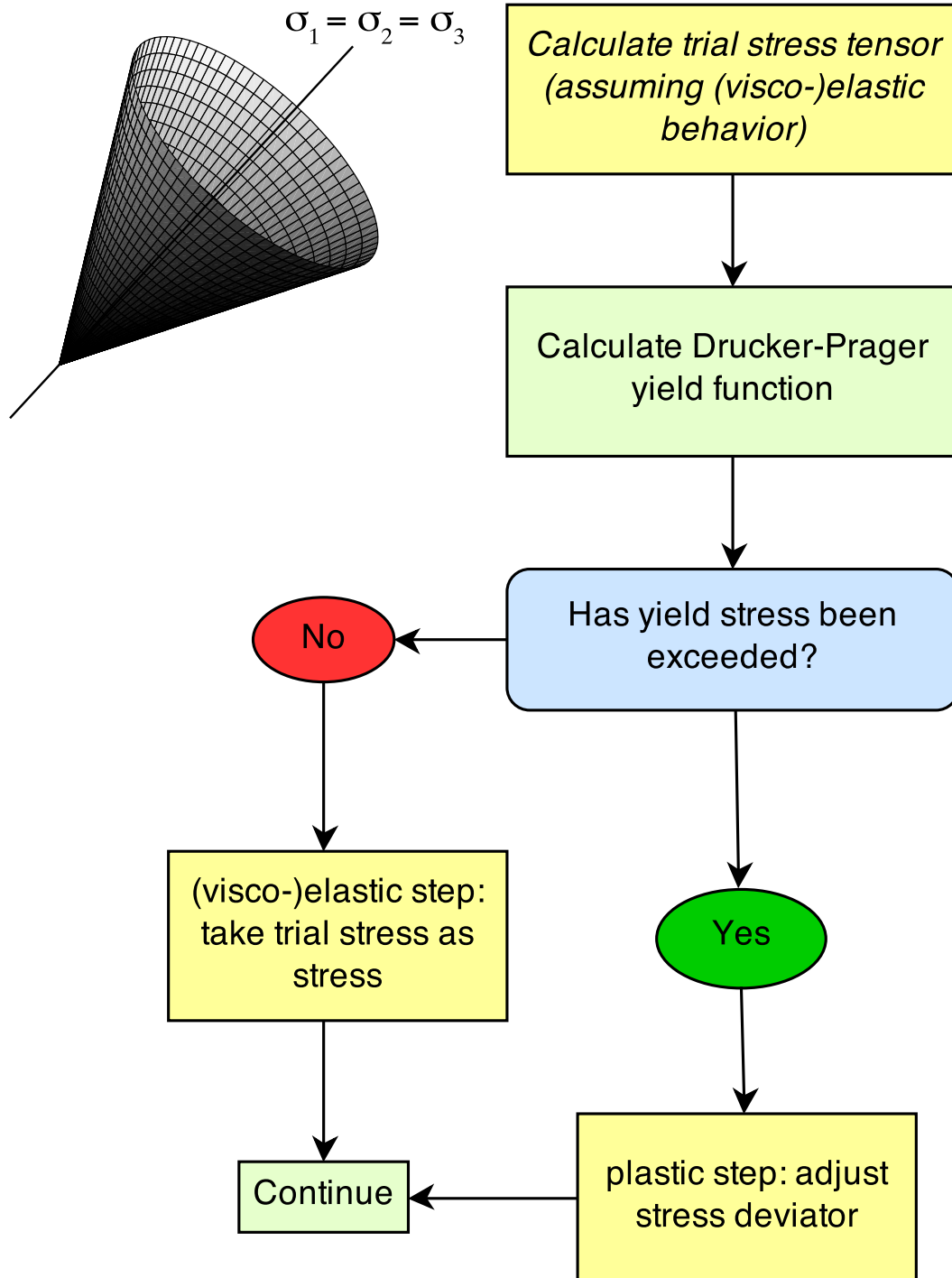
Adjusted stress:

$$\tau_{ij} = \tau_m^{\text{trial}} \delta_{ij} + r s_{ij}^{\text{trial}}$$

Yield factor r with viscoelastic relaxation time T_v :

$$r = \frac{Y(\tau^{\text{trial}})}{\sqrt{J_2(\tau^{\text{trial}})}} + \left(1 - \frac{Y(\tau^{\text{trial}})}{\sqrt{J_2(\tau^{\text{trial}})}} \right) \exp \frac{-\Delta t}{T_v}$$

Return map algorithm in AWP-ODC FD code



Yield factor r :

$$r = \frac{Y(\tau^{\text{trial}})}{\sqrt{J_2(\tau^{\text{trial}})}}$$

Adjusted stress:

$$\tau_{ij} = \tau_m^{\text{trial}} \delta_{ij} + r s_{ij}^{\text{trial}}$$

Yield factor r with viscoelastic relaxation time T_v :

$$r = \frac{Y(\tau^{\text{trial}})}{\sqrt{J_2(\tau^{\text{trial}})}} + \left(1 - \frac{Y(\tau^{\text{trial}})}{\sqrt{J_2(\tau^{\text{trial}})}} \right) \exp \frac{-\Delta t}{T_v}$$

Extra parameters for elasto-plastic simulation:

- » initial stress field τ
- » fluid pressure P_f
- » friction angle φ
- » cohesion c

Return map algorithm in AWP-ODC FD code

Current development status of plasticity in AWP-ODC code

AWP-ODC CPU



- » Drucker-Prager (DP) plasticity implemented in wave propagation and dynamic rupture mode
- » verified using SCEC/USGS rupture code verification project
- » plastic yielding requires extra communication (swapping of shear stresses before and after invoking DP subroutines)
- » DP-plasticity adds ~25% extra CPU hours (compared to viscoelastic run)
- » scalability tested on 4,000 CPU cores

Return map algorithm in AWP-ODC FD code

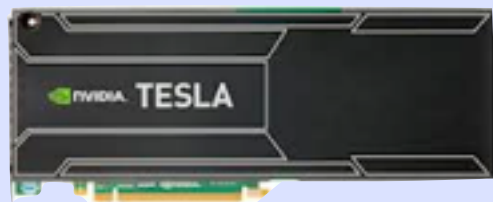
Current development status of plasticity in AWP-ODC code

AWP-ODC CPU



- » Drucker-Prager (DP) plasticity implemented in wave propagation and dynamic rupture mode
- » verified using SCEC/USGS rupture code verification project
- » plastic yielding requires extra communication (swapping of shear stresses before and after invoking DP subroutines)
- » DP-plasticity adds ~25% extra CPU hours (compared to viscoelastic run)
- » scalability tested on 4,000 CPU cores

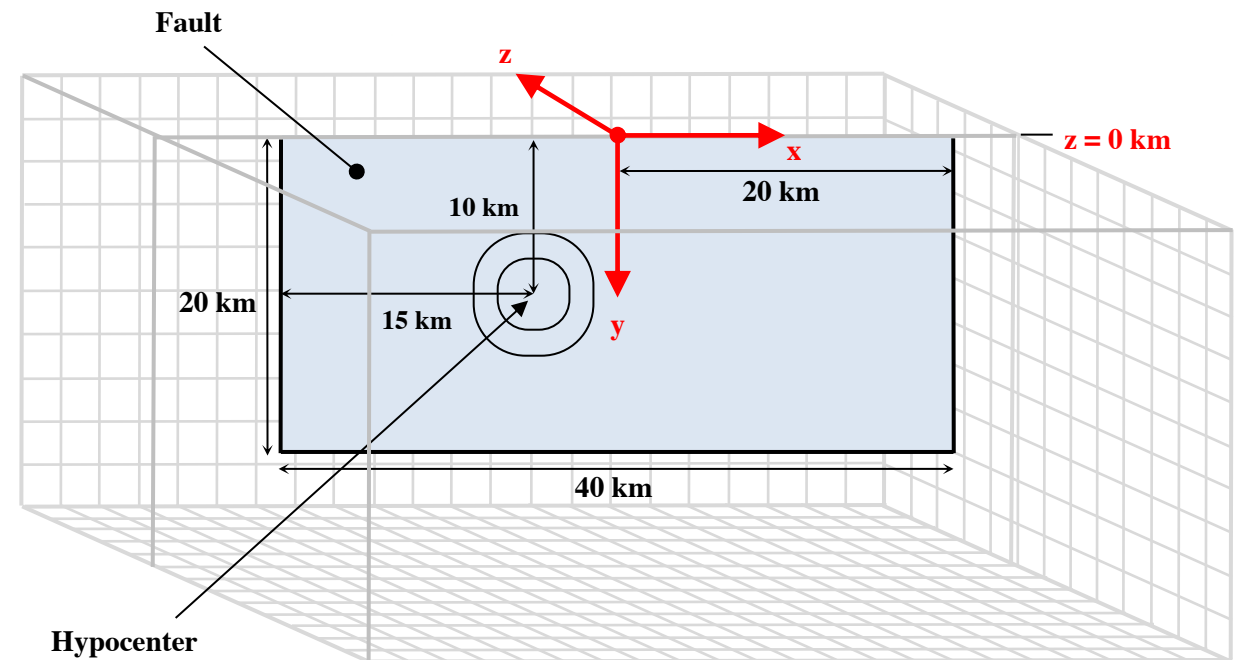
AWP-ODC GPU



- » Drucker-Prager (DP) plasticity implemented (only wave propagation available)
- » verified against AWP-ODC CPU
- » ghost cells increased from 4 to 8 layers (no extra communication required)
- » computational cost of DP-plasticity depends on dimensions of subdomain (+10% for ShakeOut-D)
- » scalability unaffected by DP computations (10,000+ GPUs)

SCEC/USGS Spontaneous Rupture Code Verification Project

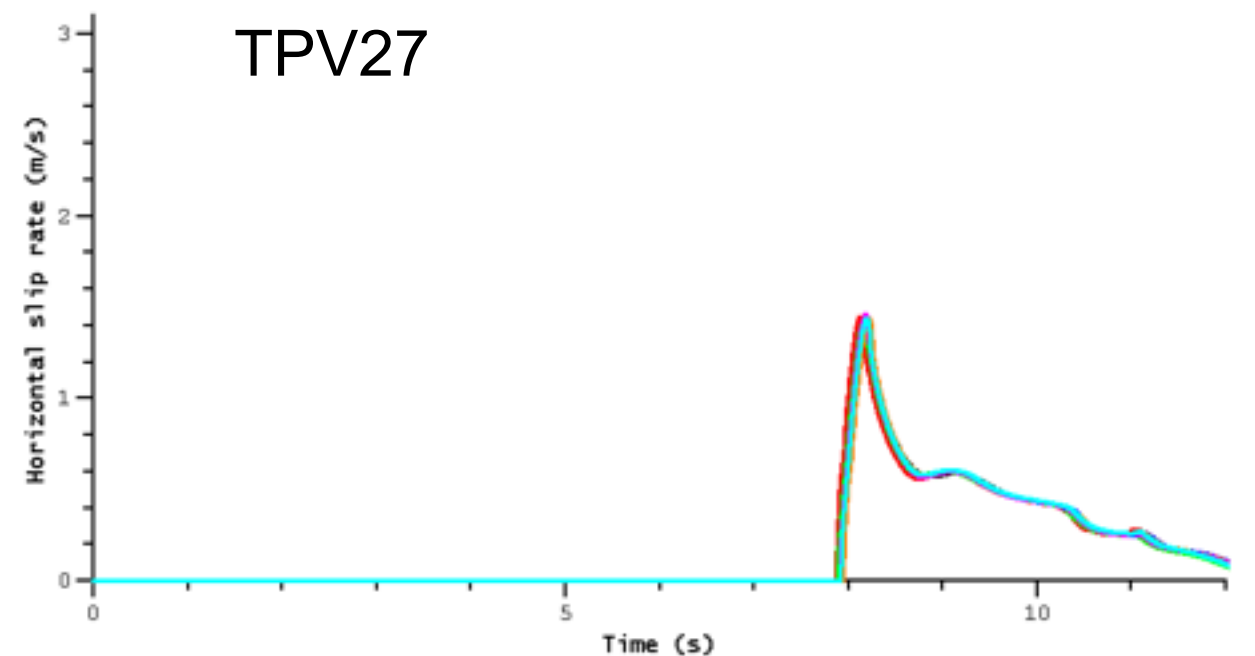
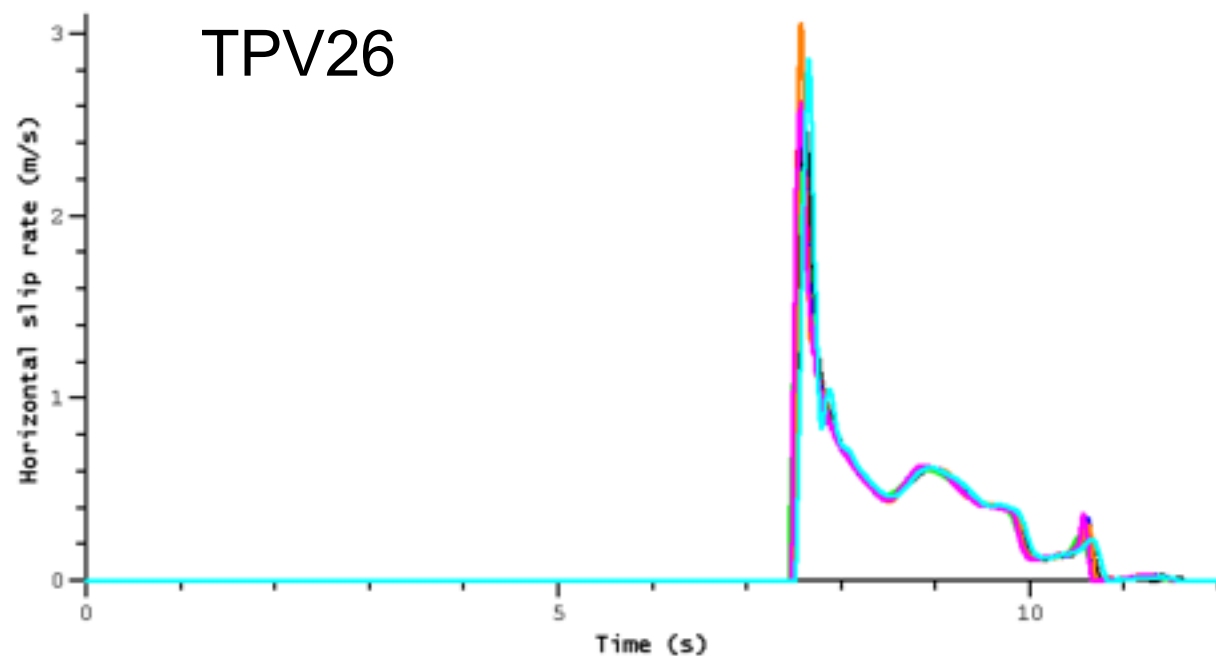
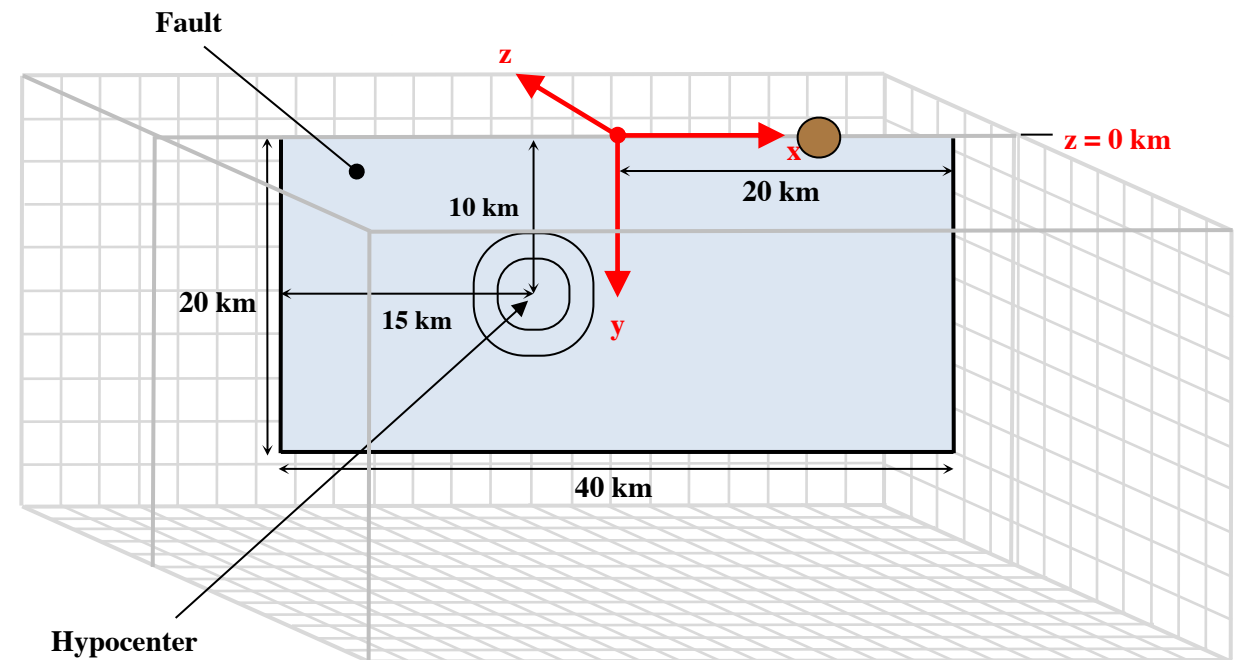
Spontaneous rupture on a vertical,
planar strike-slip fault without (TPV26)
and with (TPV27) plasticity



SCEC/USGS Spontaneous Rupture Code Verification Project

Spontaneous rupture on a vertical, planar strike-slip fault without (TPV26) and with (TPV27) plasticity

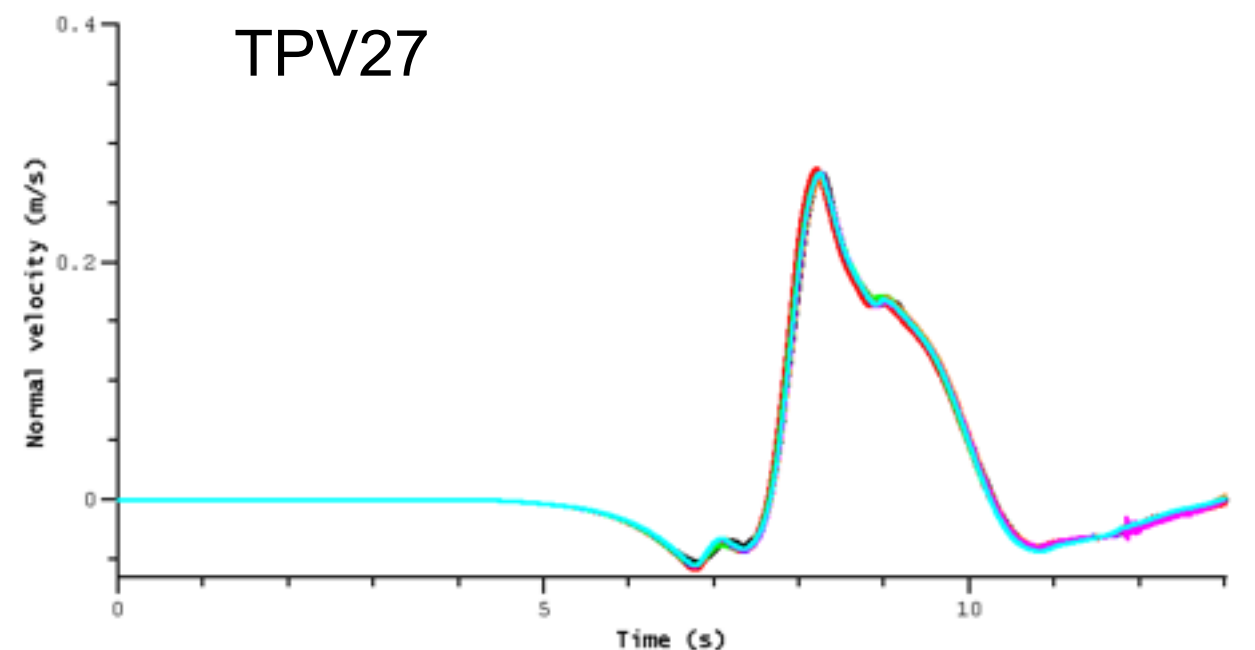
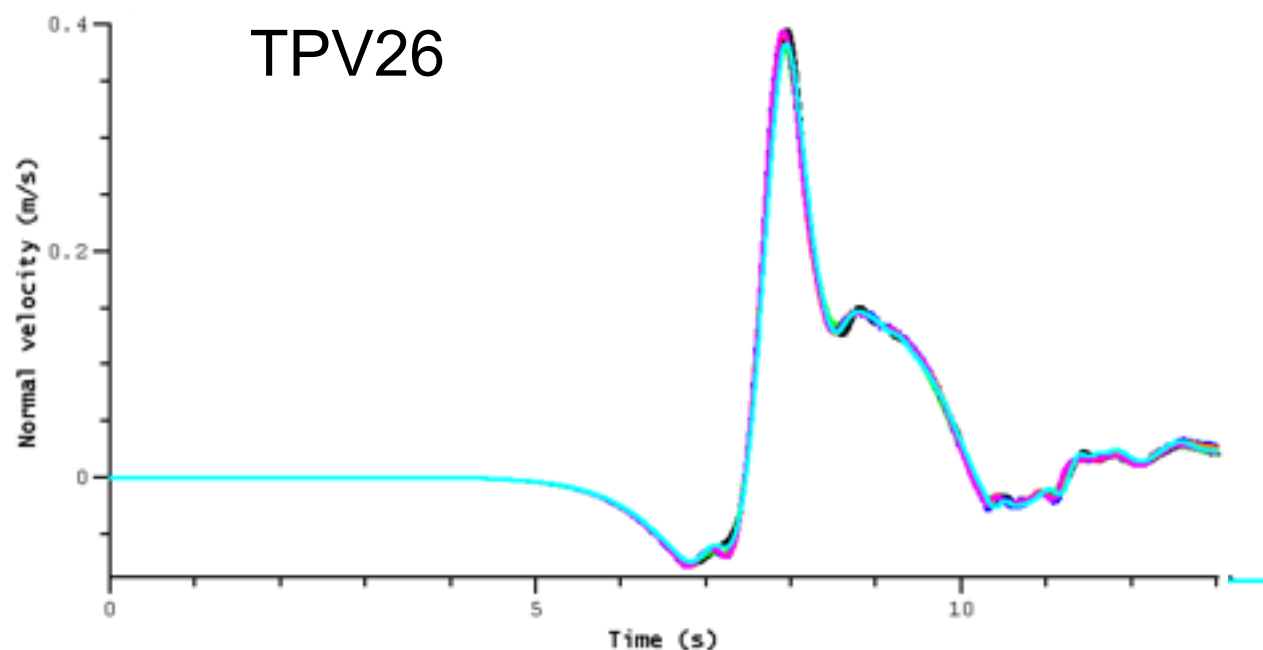
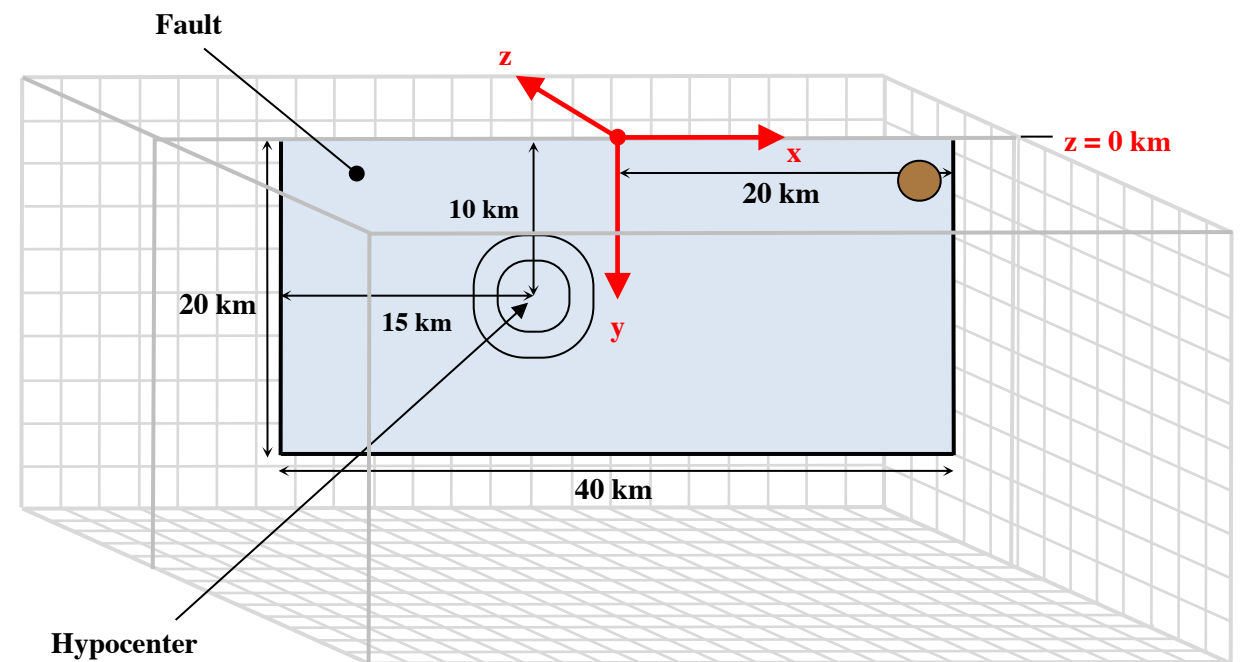
—	barall.2 (Michael Barall - FaultMod - 50 m)
—	chen.2 (Xiaofei Chen - Finite Difference Method - CGFDM - 50 m)
—	duan.2 (Benchun Duan - Finite Element - EQdyna - 50 m)
—	kaneko.2 (Yoshihiro Kaneko - Spectral Element - SPECFEM3D - 50m)
—	ma.2 (Shuo Ma - Finite Element - MAFE (50 m))
—	roten.3 (Daniel Roten - Finite Difference - AWM - 25 m)
—	shi.3 (Zheqiang Shi - Generalized Finite Difference - SORD - 25 m)



SCEC/USGS Spontaneous Rupture Code Verification Project

Spontaneous rupture on a vertical, planar strike-slip fault without (TPV26) and with (TPV27) plasticity

—	barall.2 (Michael Barall - FaultMod - 50 m)
—	chen.2 (Xiaofei Chen - Finite Difference Method - CGFDM - 50 m)
—	duan.2 (Benchun Duan - Finite Element - EQdyna - 50 m)
—	kaneko.2 (Yoshihiro Kaneko - Spectral Element - SPECFEM3D - 50m)
—	ma.2 (Shuo Ma - Finite Element - MAFE (50 m))
—	roten.3 (Daniel Roten - Finite Difference - AWM - 25 m)
—	shi.3 (Zheqiang Shi - Generalized Finite Difference - SORD - 25 m)

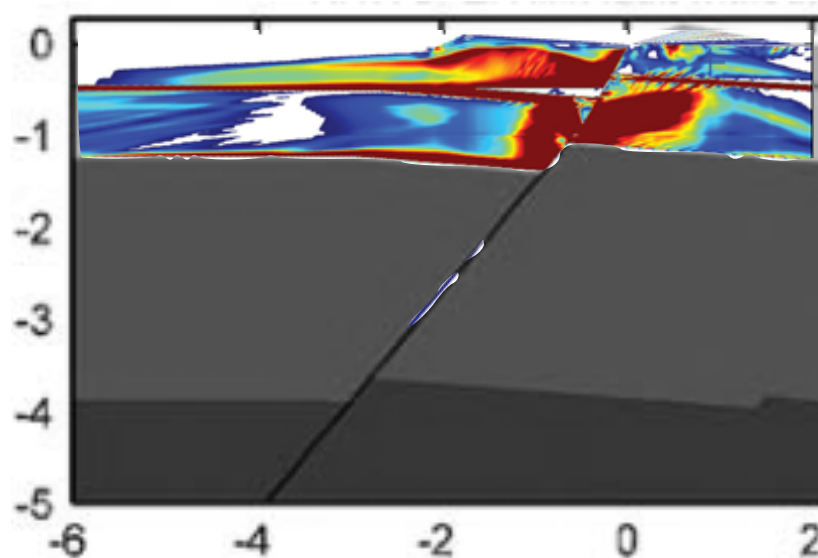


ShakeOut Scenario w/ Plasticity

Motivation

- » Waveguide amplification could cause damaging long-period ground motion in LAB
- » Evidence for waveguide from both numerical simulations and virtual earthquakes derived from ambient noise (Denolle *et al.*, 2014)
- » Previous simulations assumed a **linear** stress-strain relationship in crustal and sedimentary rocks
- » Amplifications predicted from ambient noise are also inherently **linear**
- » However, **nonlinear** material behavior may occur near the source (off-fault plasticity), along the path and at the site
- » We study effect of nonlinearity by simulating ShakeOut earthquake scenarios for a medium governed by Drucker-Prager elastoplasticity

Off-fault plasticity

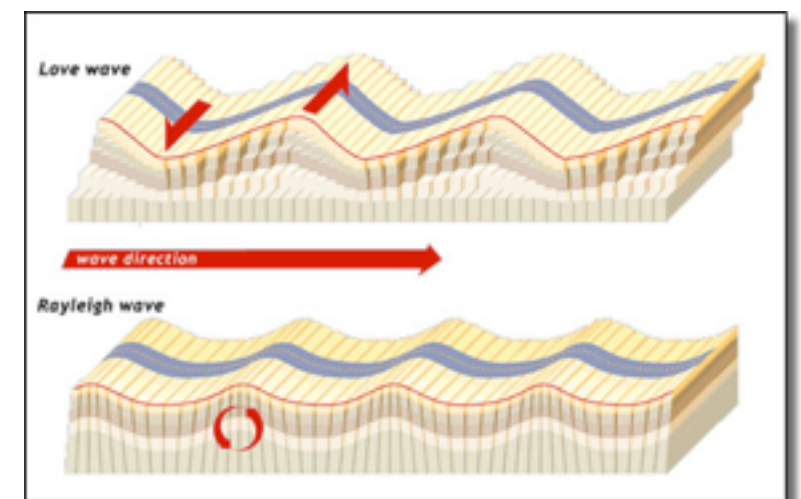


Duan & Day (2010)

Nonlinear soil behavior



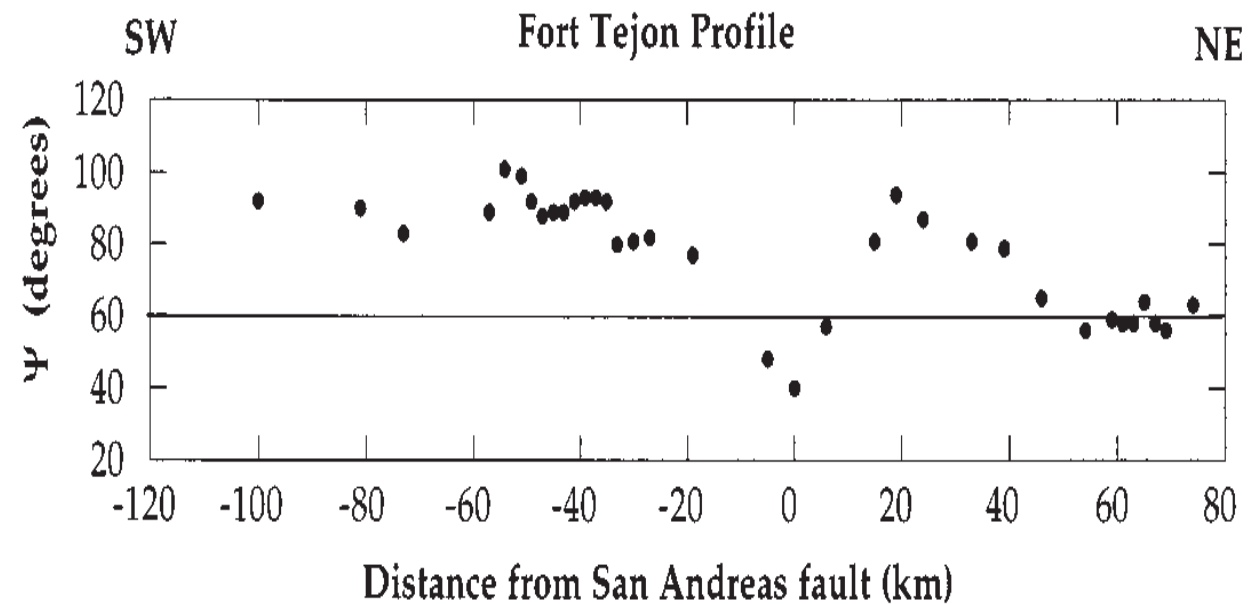
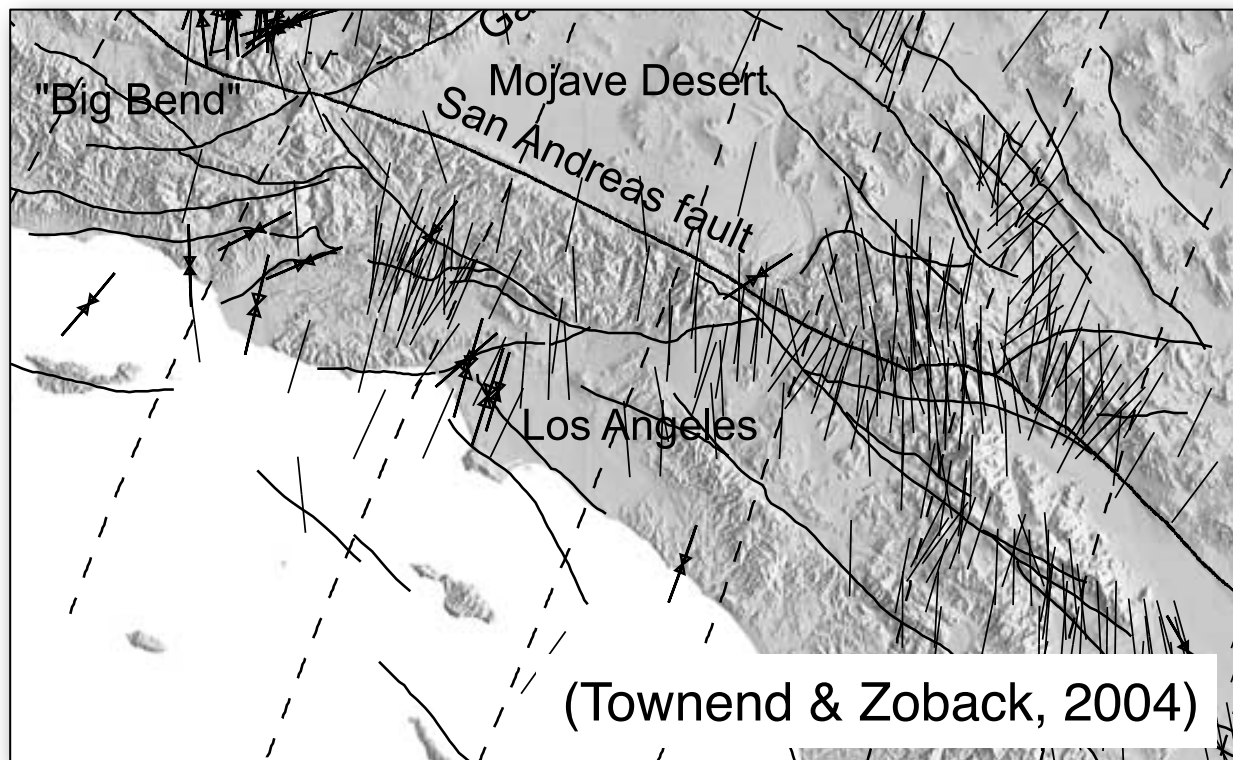
Nonlinear attenuation of surface waves



Sleep & Erickson (2014)

ShakeOut Scenario w/ Plasticity

Definition of initial stress field



Scholz (2000)

Initial stress model A

- $P_f = g \rho_w z$
- $\tau_{zz} = g \int_0^z \rho(z) dz$
- σ_2 is vertical
- σ_1 points to N22°E
- $\sigma_1 = \frac{4}{3}\sigma_2 = \frac{2}{3}\sigma_3$

Initial stress model B

- $P_f = g \rho_w z$
- $\tau_{zz} = g \int_0^z \rho(z) dz$
- σ_2 is vertical
- σ_1 points to N7.5°W
- $\sigma_1 = \frac{4}{3}\sigma_2 = \frac{2}{3}\sigma_3$

Initial stress model C

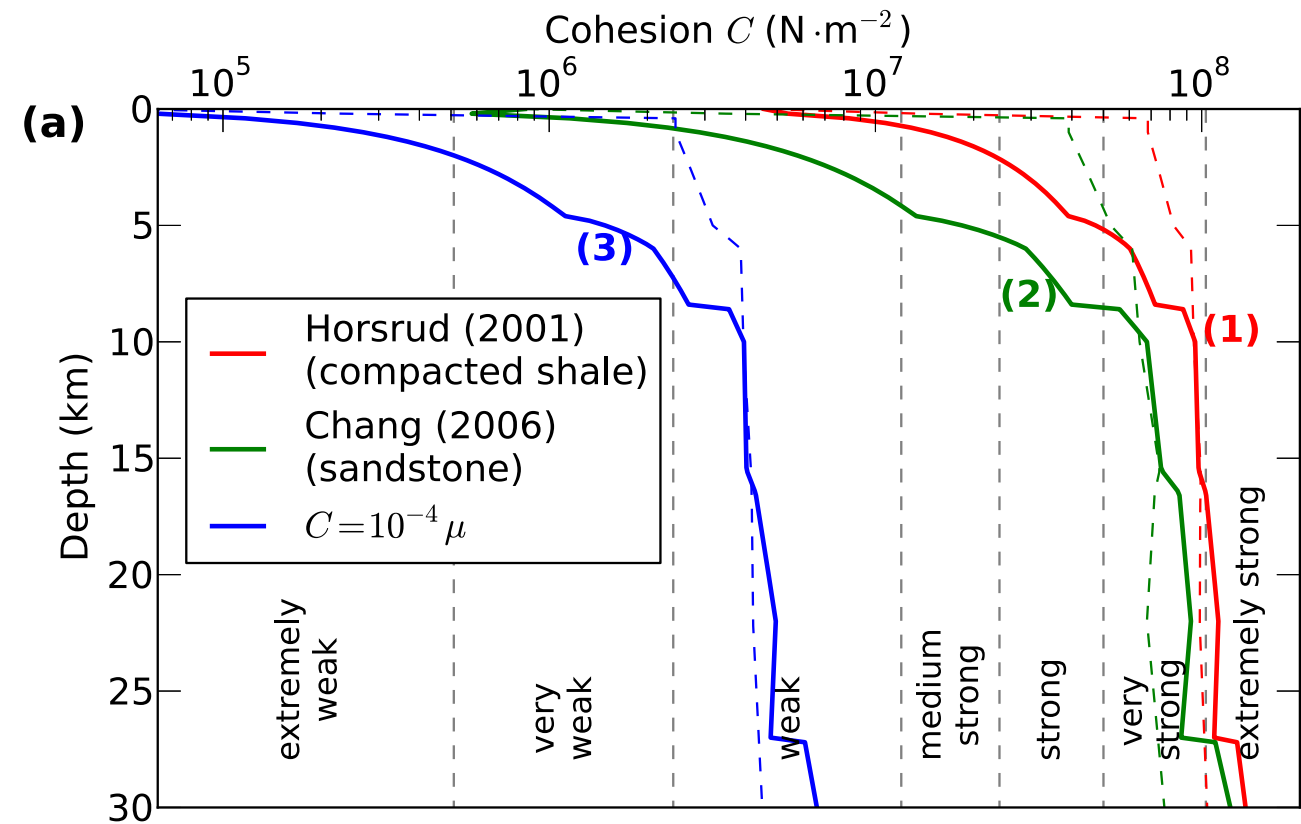
- $P_f = g \rho_w z$
- $\tau_{zz} = g \int_0^z \rho(z) dz$
- $\tau_{xx} = \tau_{yy} = \tau_{zz}$
- $\tau_{xy} = \tau_{xz} = \tau_{yz} = 0$

ShakeOut Scenario w/ Plasticity

Definition of rock strength

- » Petroleum industry equations predict $S_u = 2 c$ from known properties, e.g.:
- » We tested 3 different cohesion models :
 1. *compacted shale* (Horsrud *et al.*, 2001):
 2. *sandstone* (Chang *et al.*, 2006):
 3. *shallow sediments, damage zone*:
- » Friction angle:

$$\varphi = \begin{cases} 35^\circ & \text{if } V_s \leq 2500 \text{ m} \cdot \text{s}^{-1} \\ 45^\circ & \text{if } V_s > 2500 \text{ m} \cdot \text{s}^{-1} \end{cases}$$

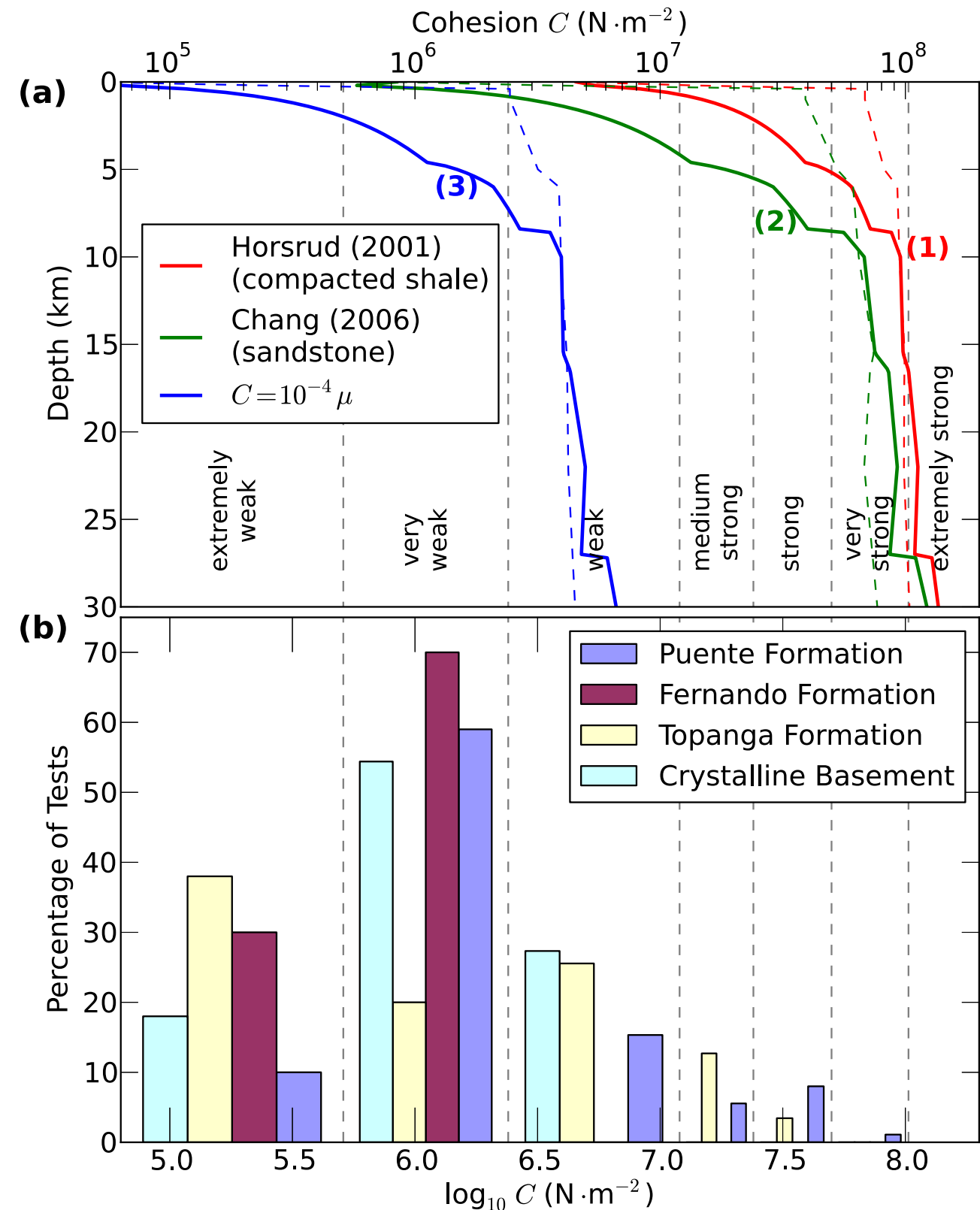


ShakeOut Scenario w/ Plasticity

Definition of rock strength

- » Petroleum industry equations predict $S_u = 2 c$ from known properties, e.g.:
- » We tested 3 different cohesion models :
 1. *compacted shale* (Horsrud *et al.*, 2001):
 2. *sandstone* (Chang *et al.*, 2006):
 3. *shallow sediments, damage zone*:
- » Friction angle:

$$\varphi = \begin{cases} 35^\circ & \text{if } V_s \leq 2500 \text{ m} \cdot \text{s}^{-1} \\ 45^\circ & \text{if } V_s > 2500 \text{ m} \cdot \text{s}^{-1} \end{cases}$$

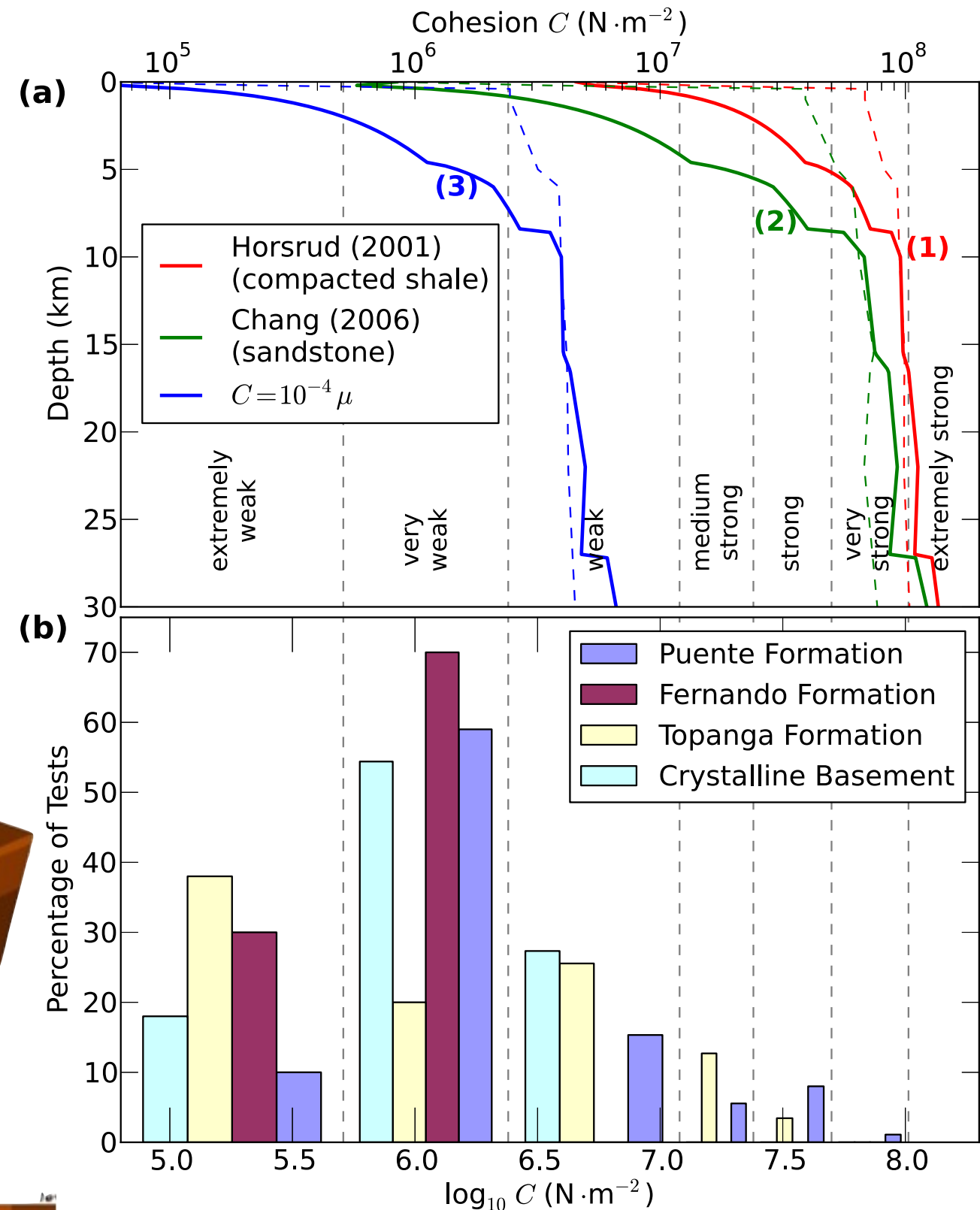
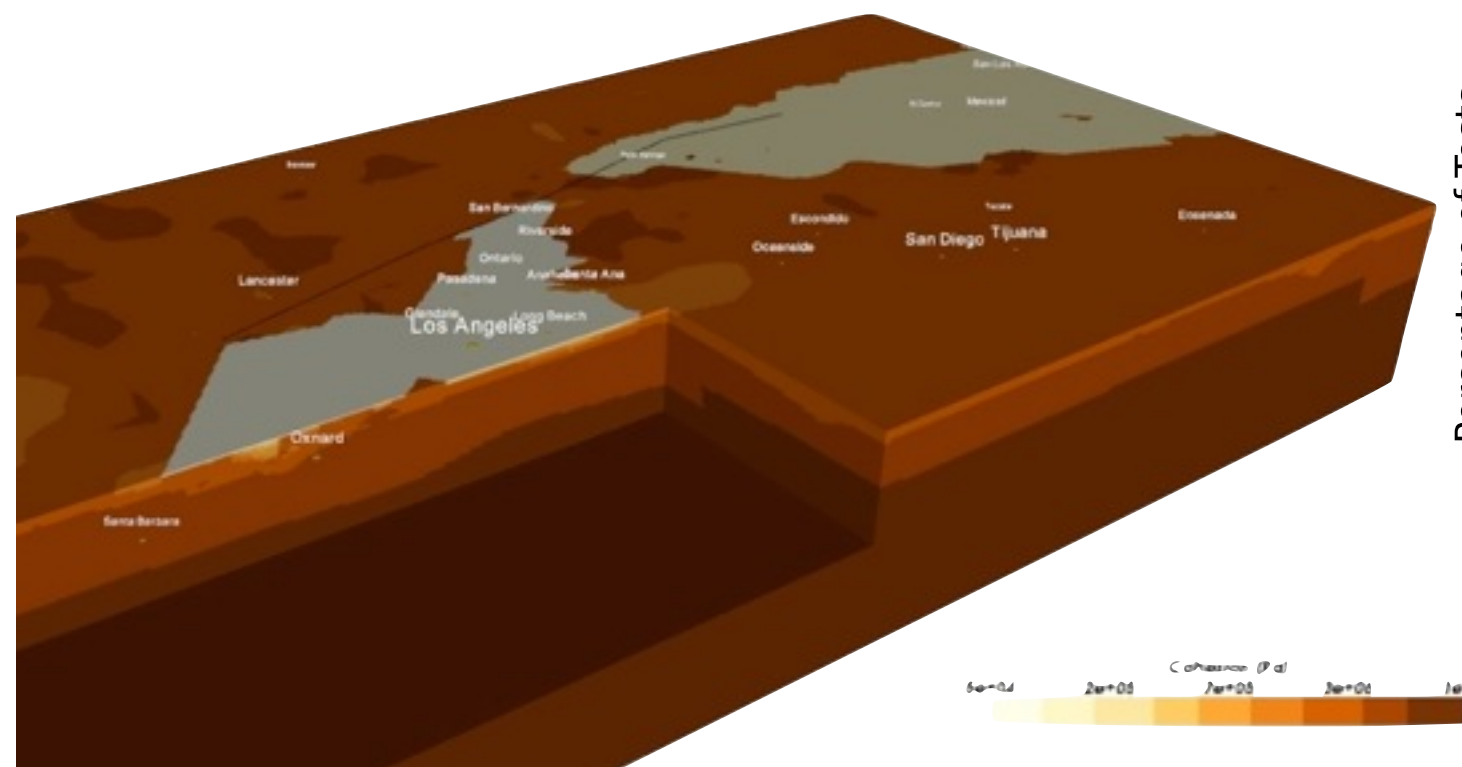


ShakeOut Scenario w/ Plasticity

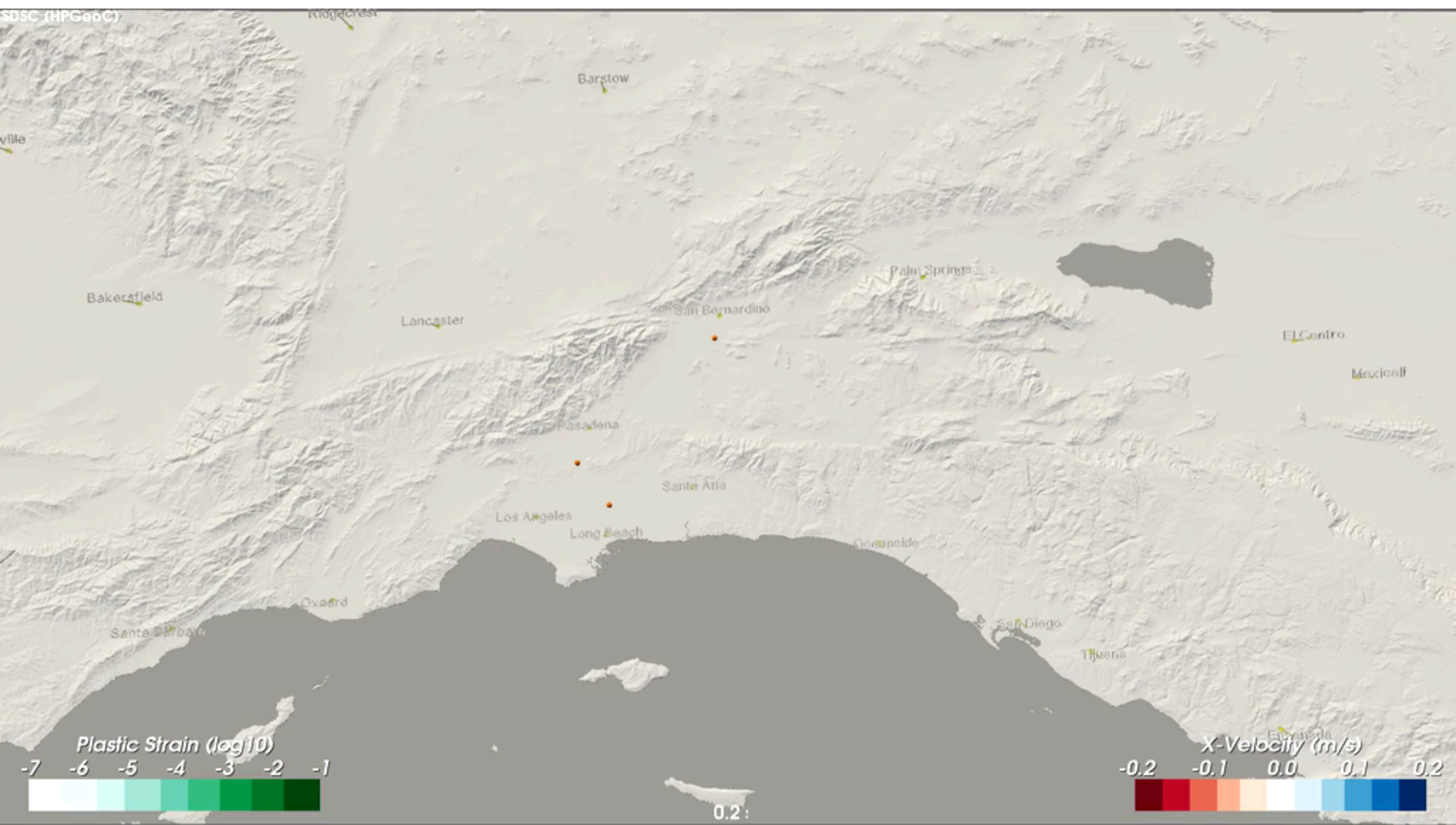
Definition of rock strength

- » Petroleum industry equations predict $S_u = 2c$ from known properties, e.g.:
- » We tested 3 different cohesion models :
 1. *compacted shale* (Horsrud *et al.*, 2001):
 2. *sandstone* (Chang *et al.*, 2006):
 3. *shallow sediments, damage zone*:
- » Friction angle:

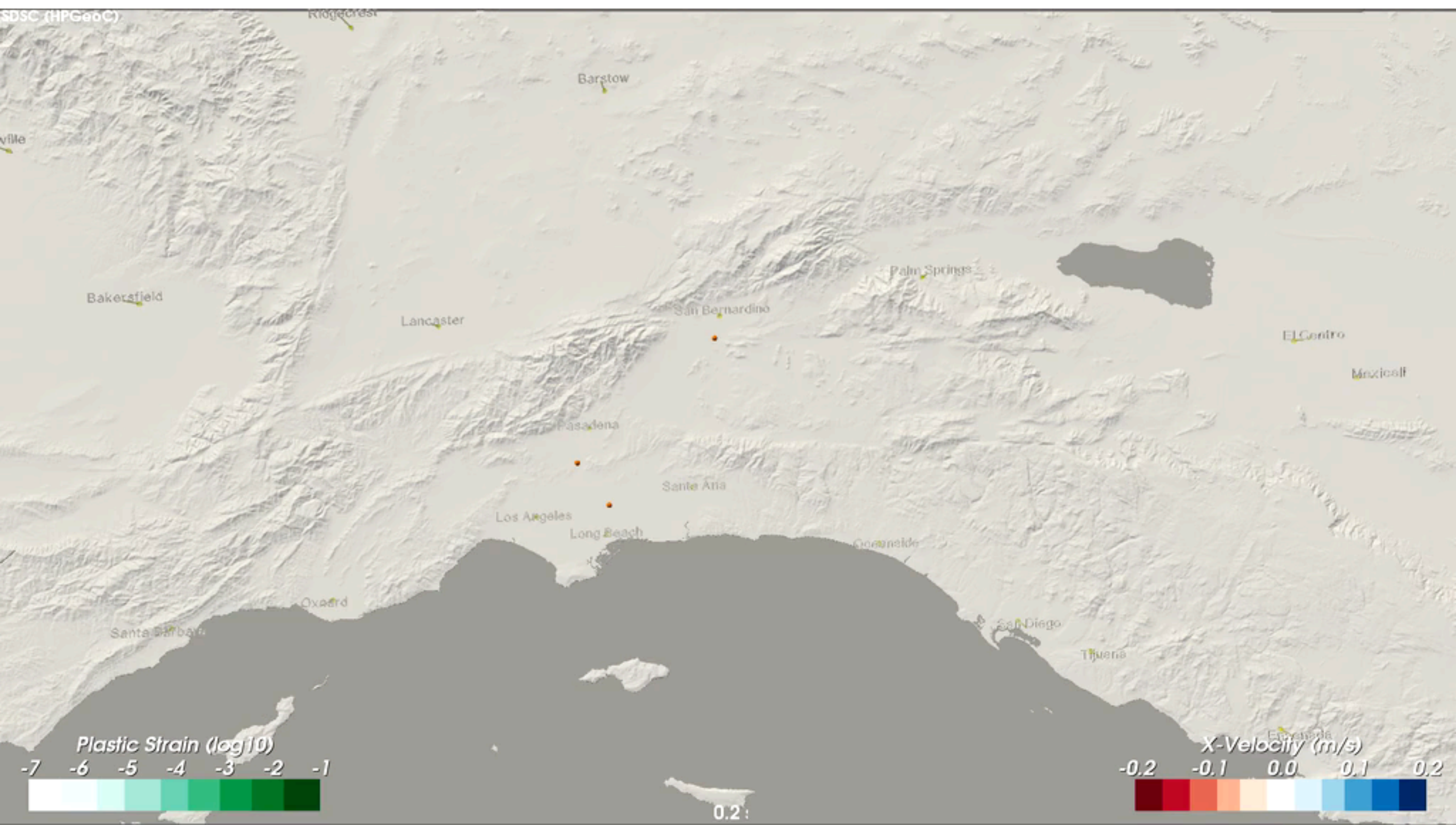
$$\varphi = \begin{cases} 35^\circ & \text{if } V_s \leq 2500 \text{ m} \cdot \text{s}^{-1} \\ 45^\circ & \text{if } V_s > 2500 \text{ m} \cdot \text{s}^{-1} \end{cases}$$



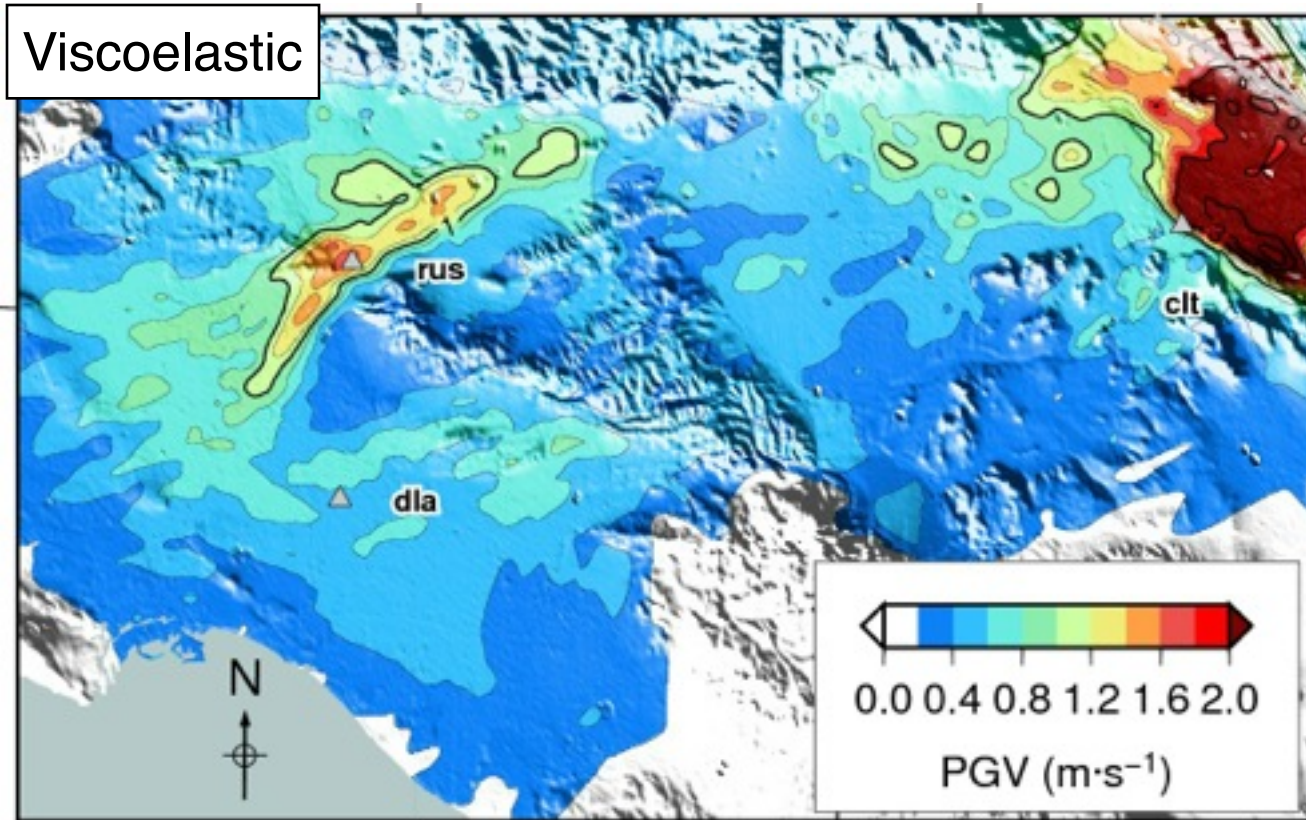
ShakeOut-D w/ plasticity (source g3d7, cohesion model 3, initial stress model A)



ShakeOut-D w/ plasticity (source g3d7, cohesion model 3, initial stress model A)

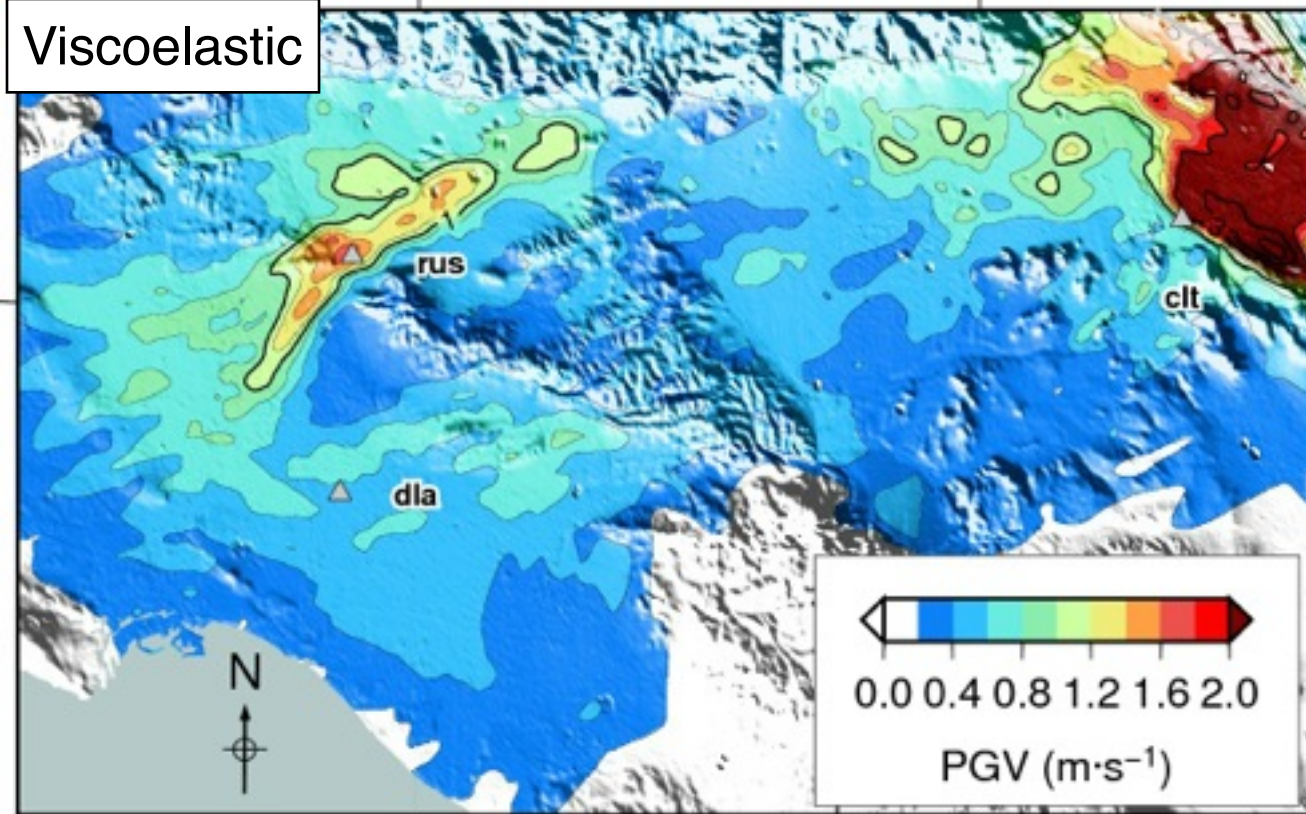


ShakeOut Scenario w/ Plasticity

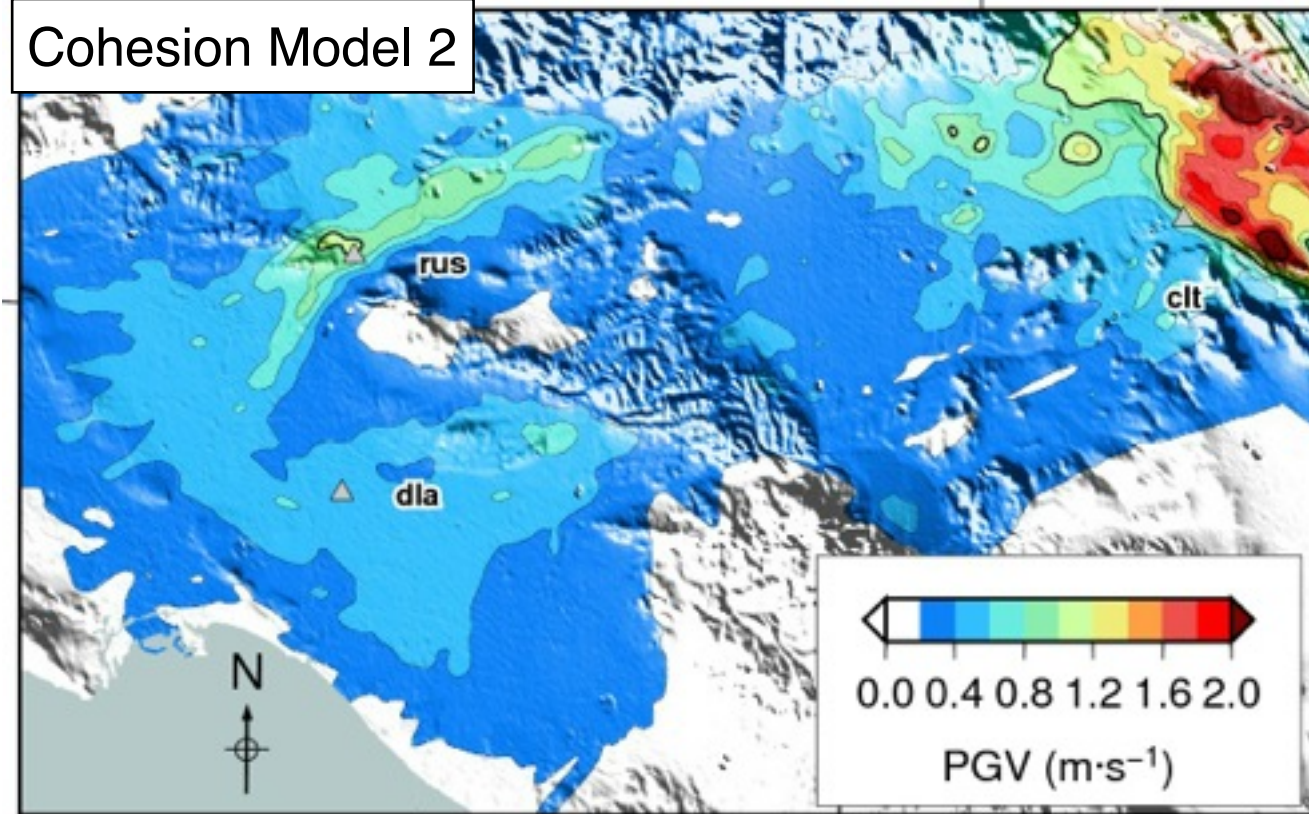


ShakeOut Scenario w/ Plasticity

Viscoelastic

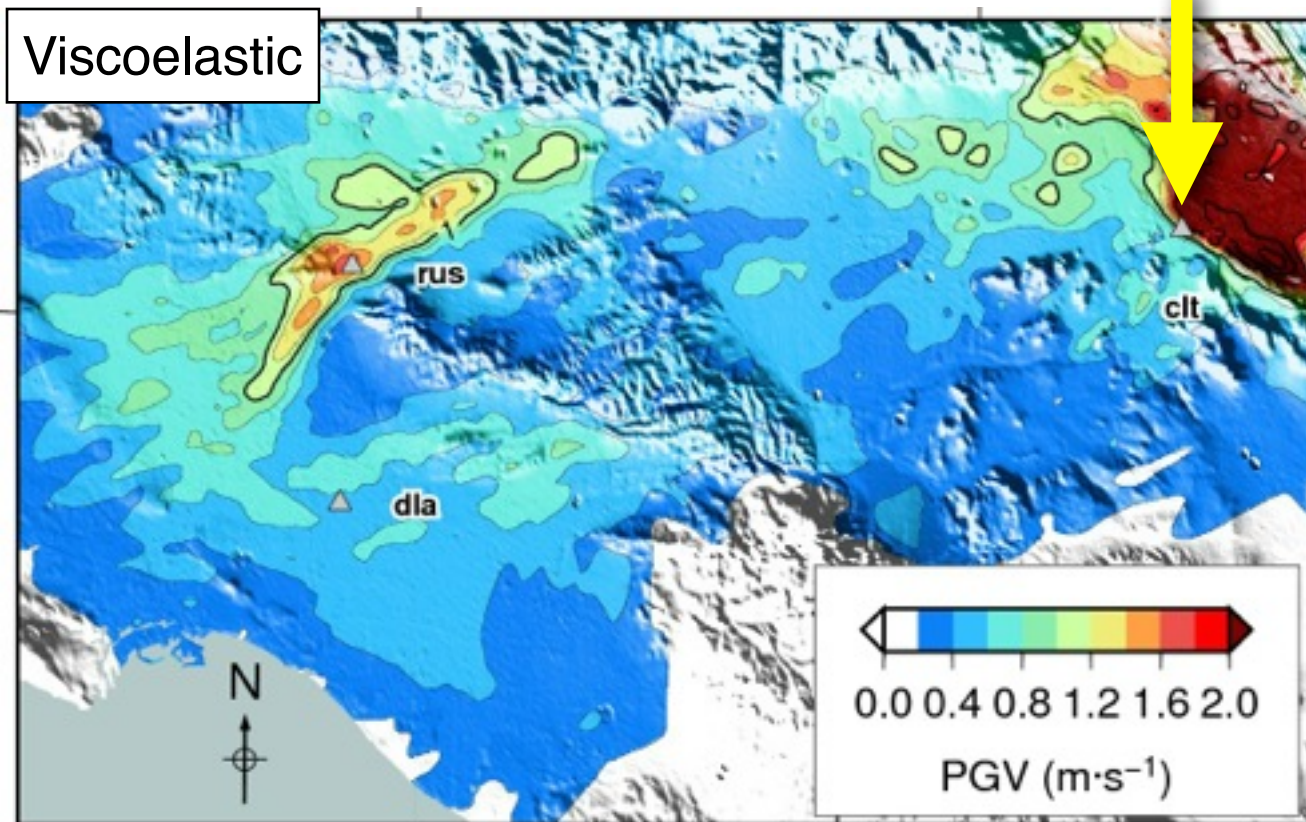


Cohesion Model 2

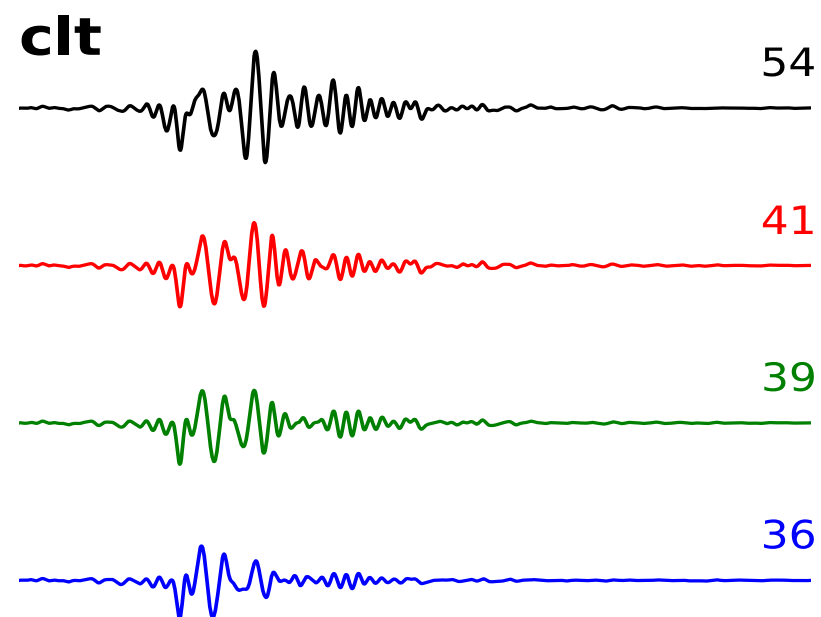
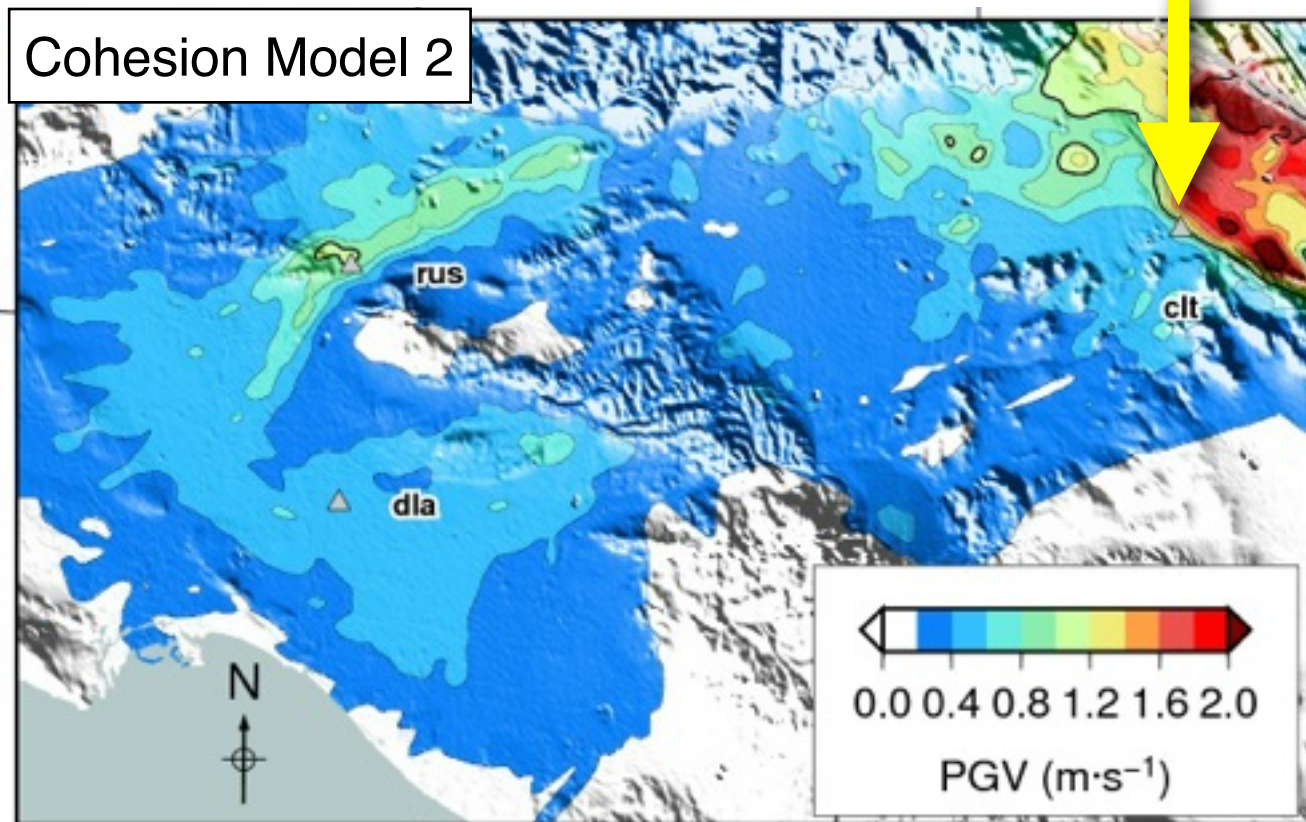


ShakeOut Scenario w/ Plasticity

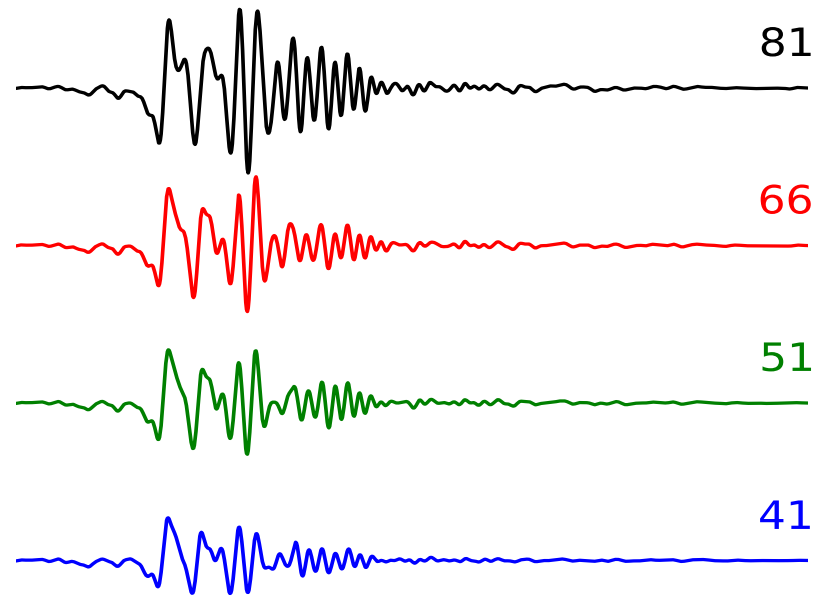
Viscoelastic



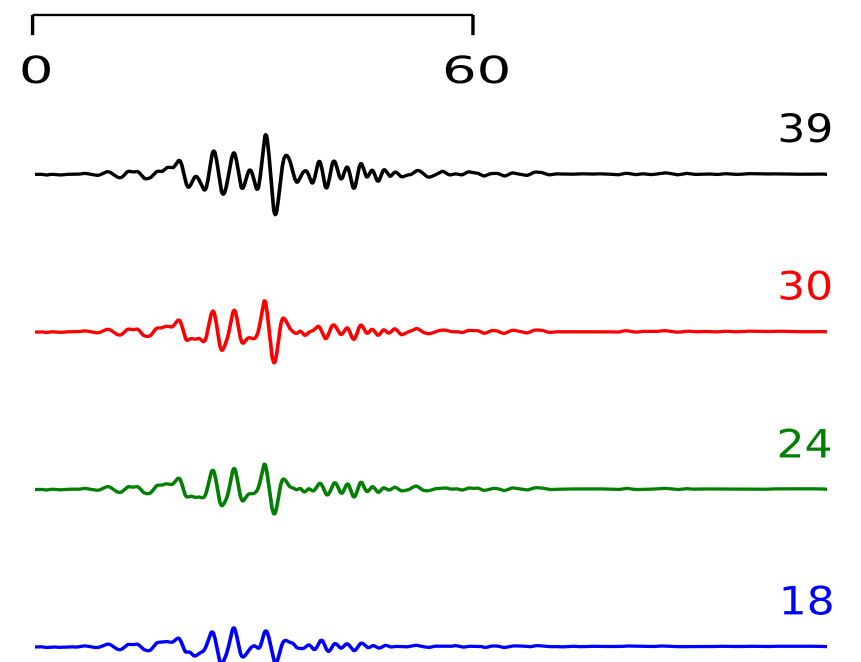
Cohesion Model 2



N130° E

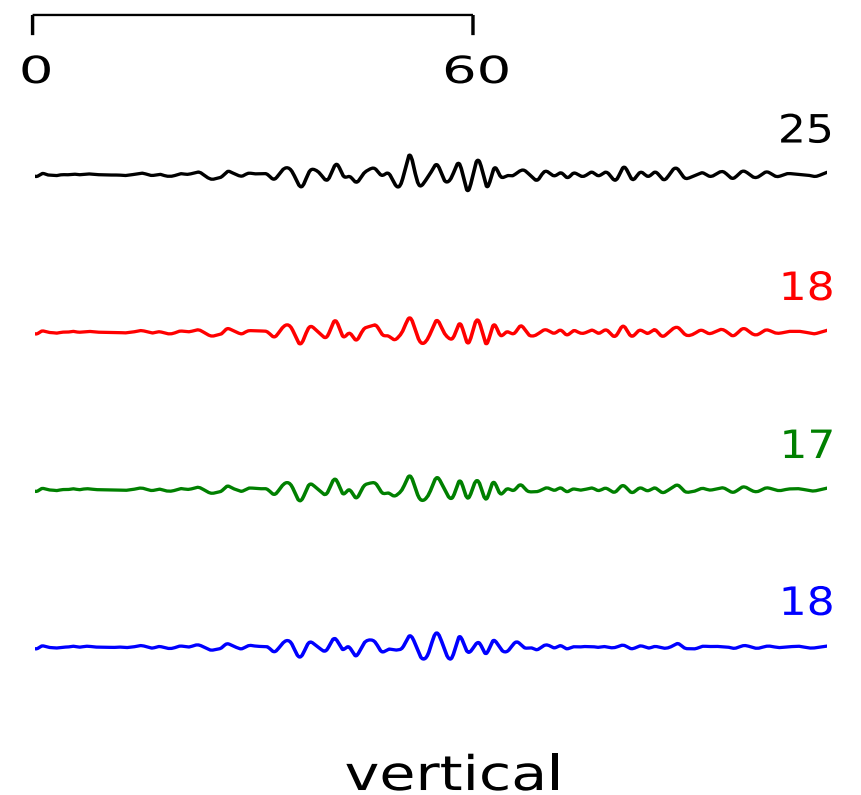
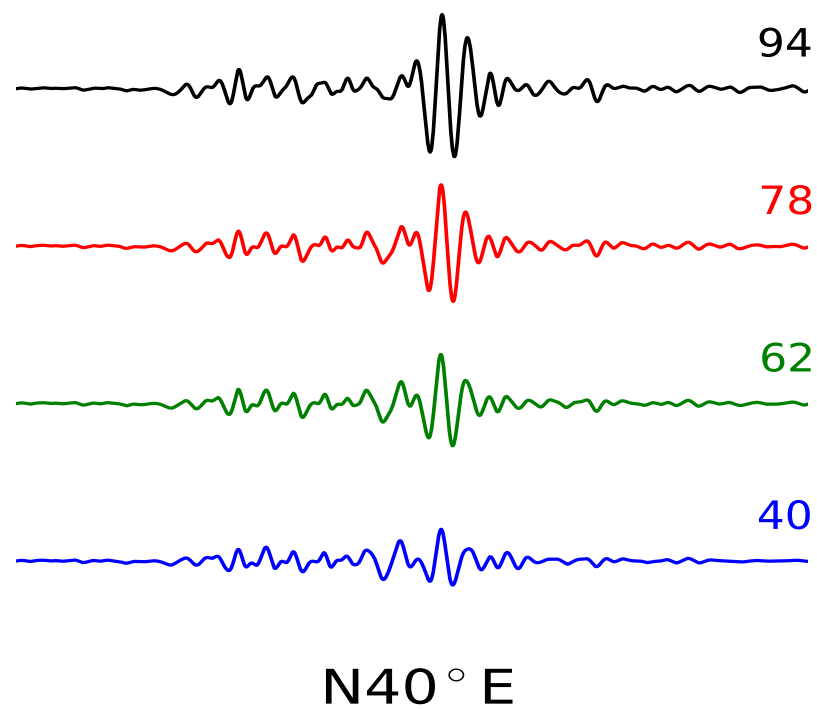
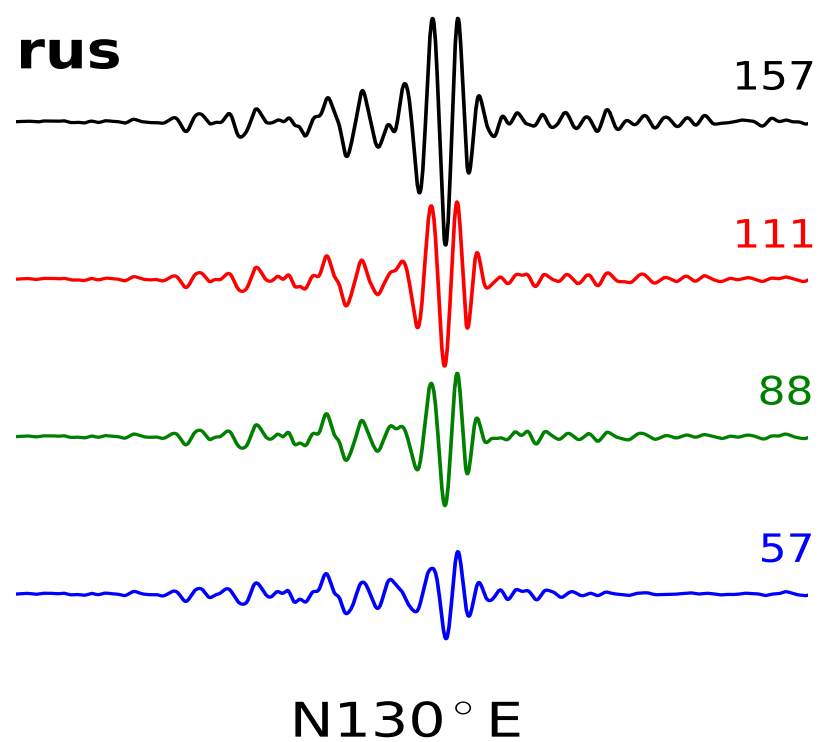
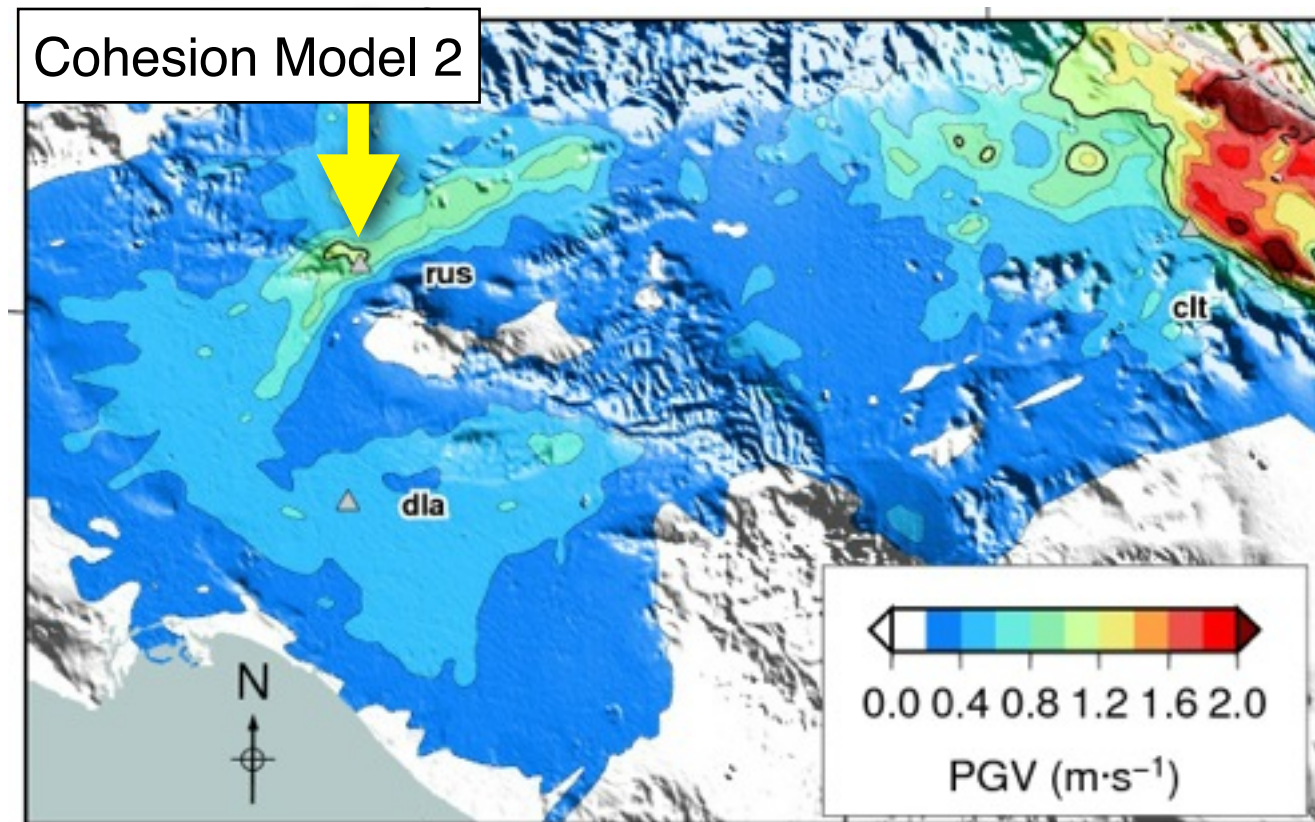
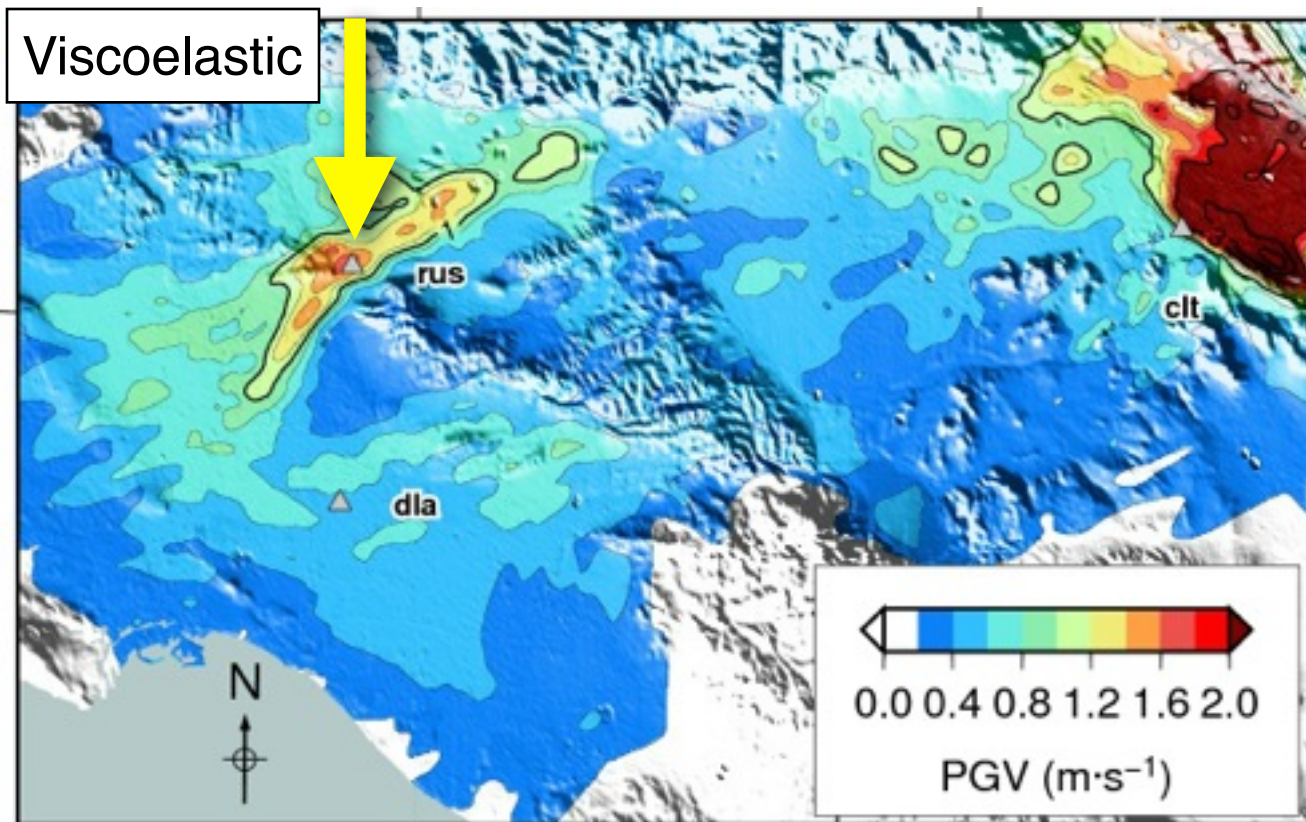


N40° E

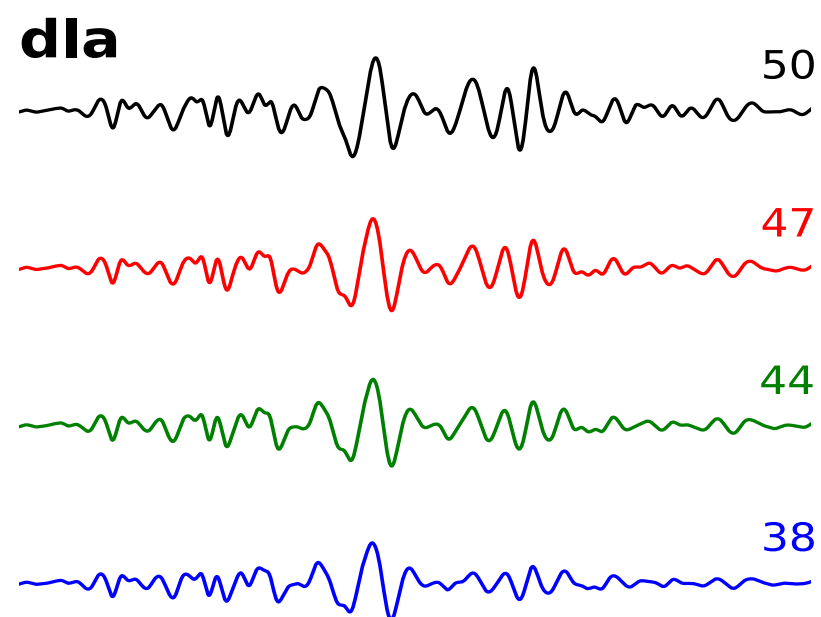
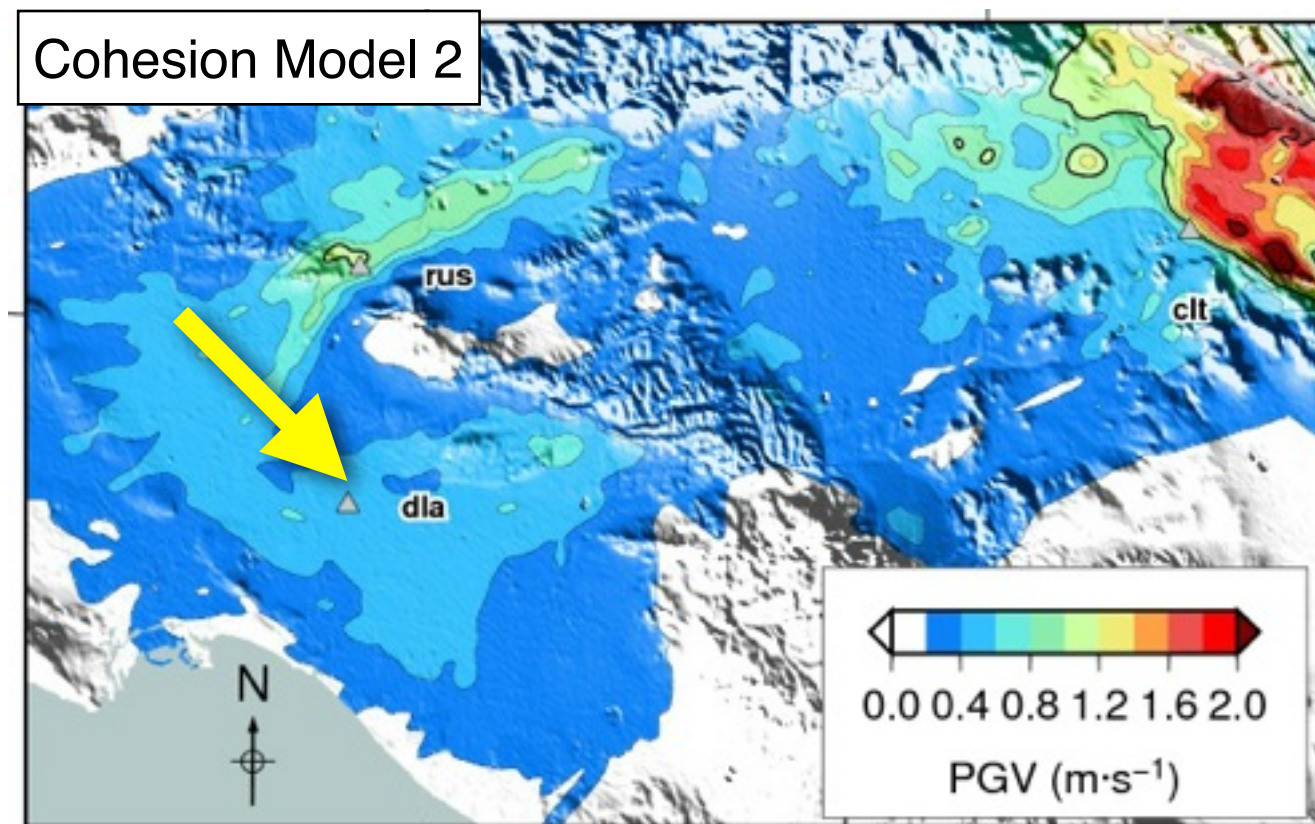
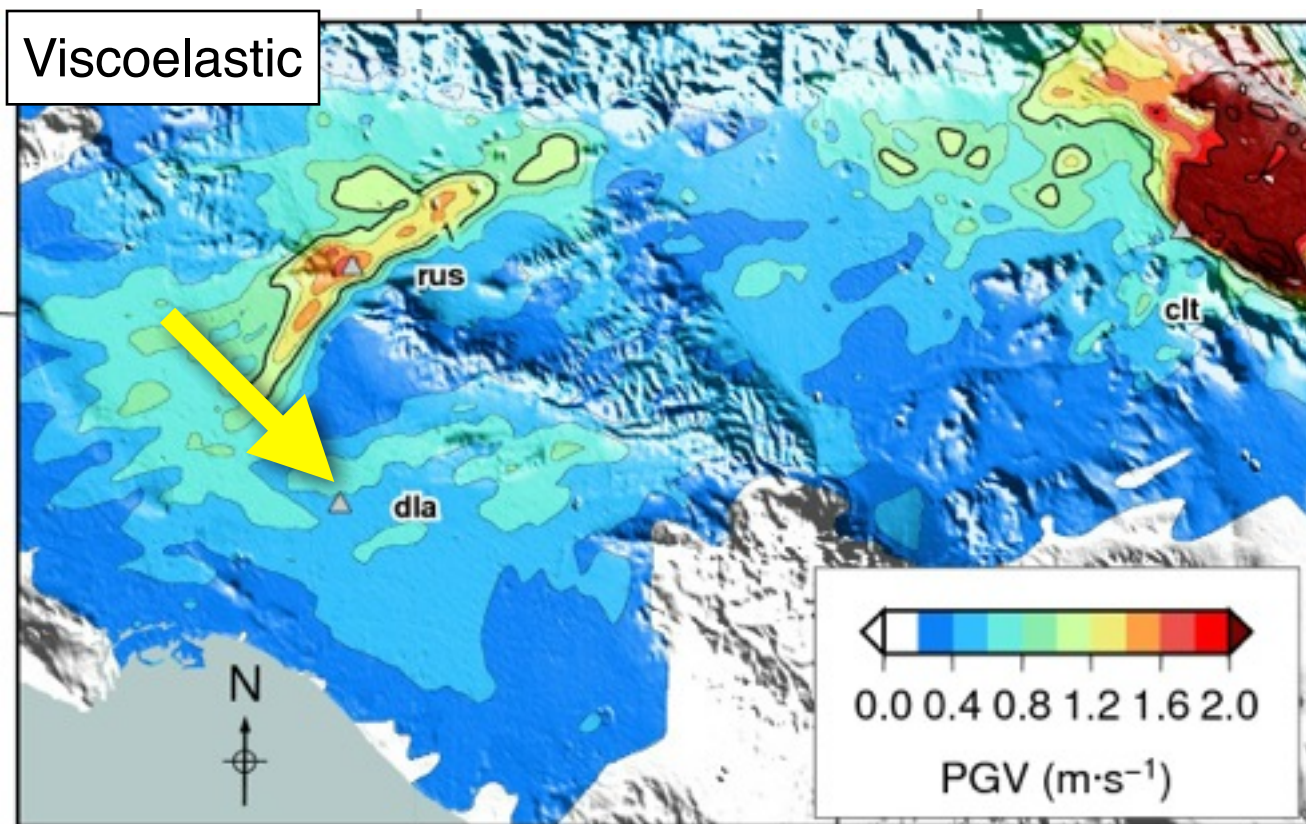


vertical

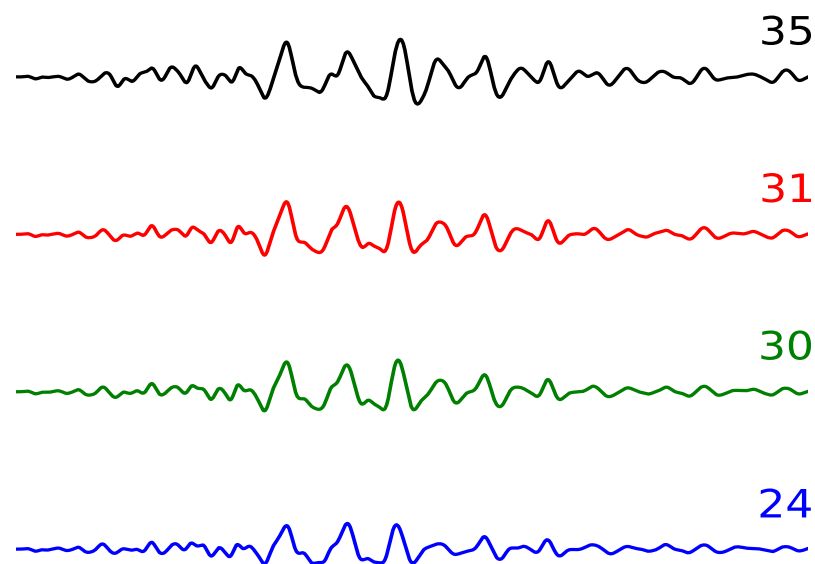
ShakeOut Scenario w/ Plasticity



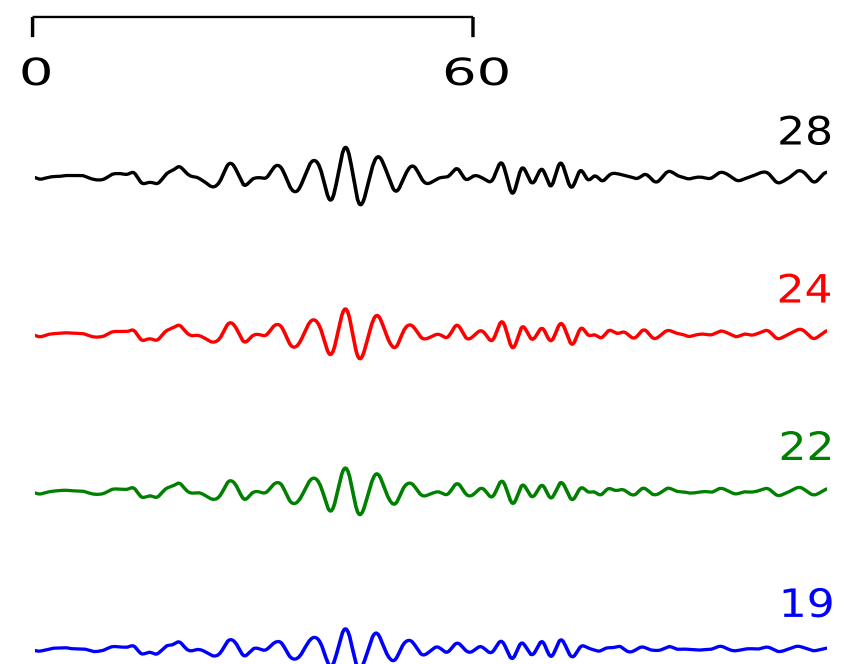
ShakeOut Scenario w/ Plasticity



N130° E

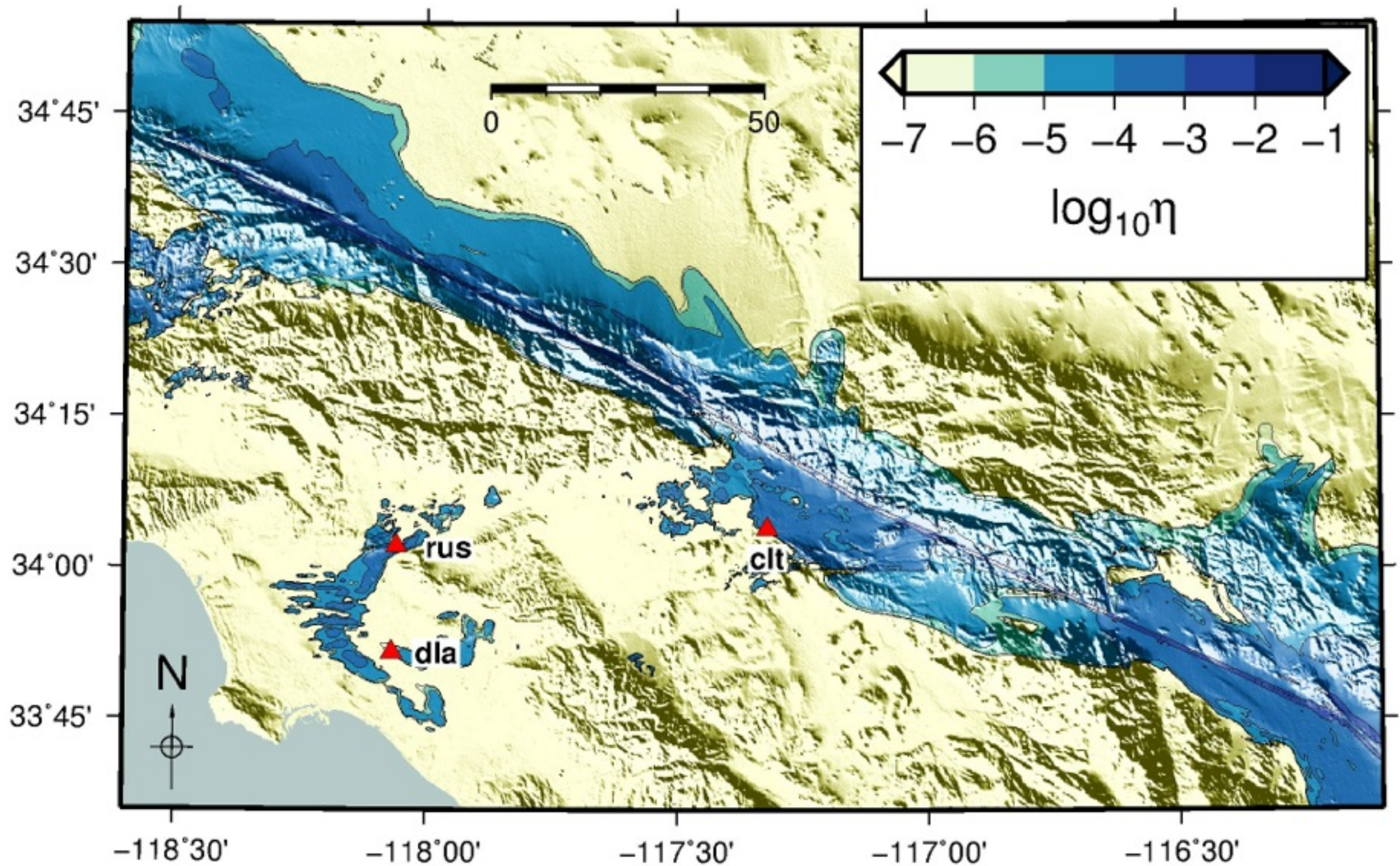


N40° E

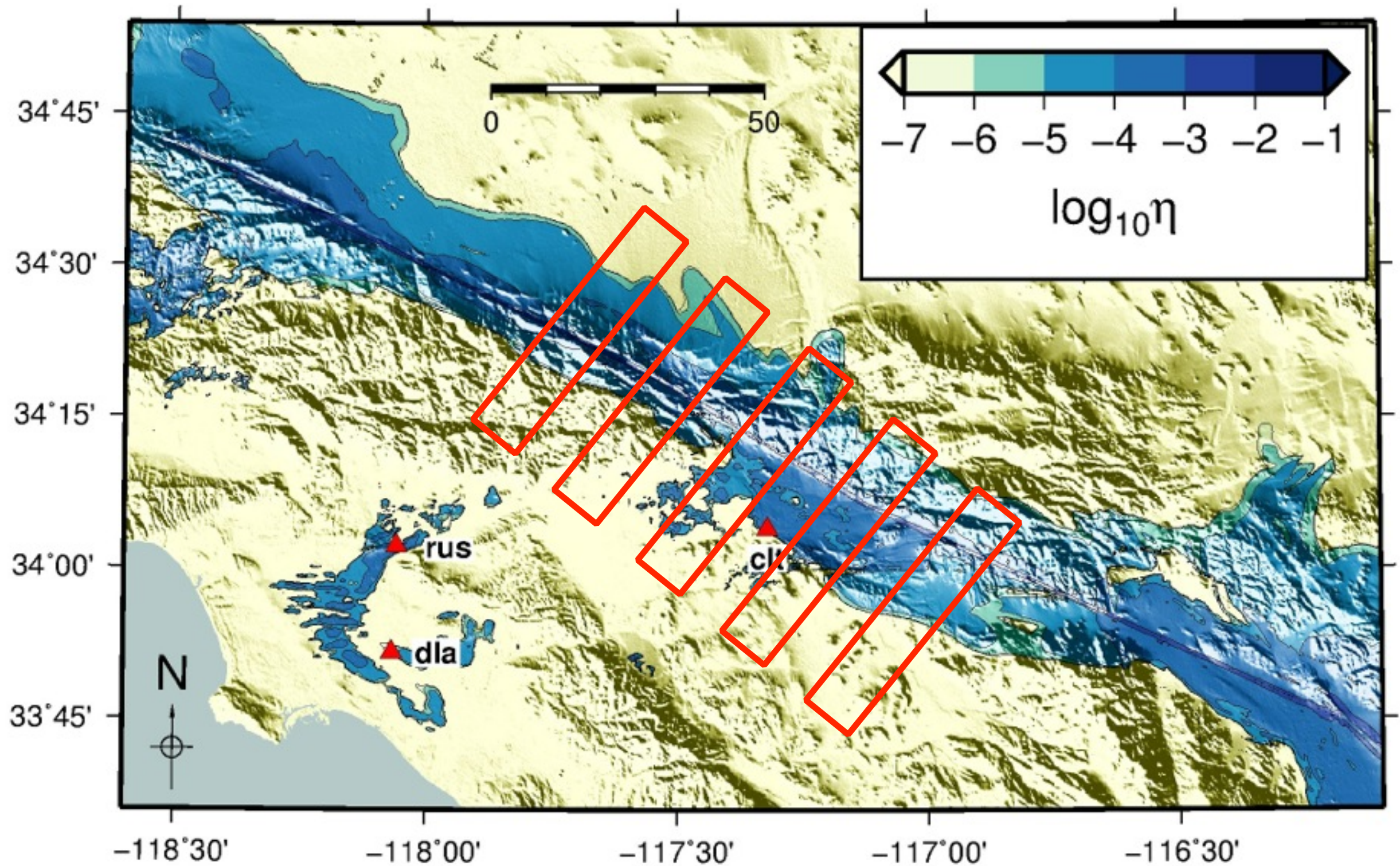


vertical

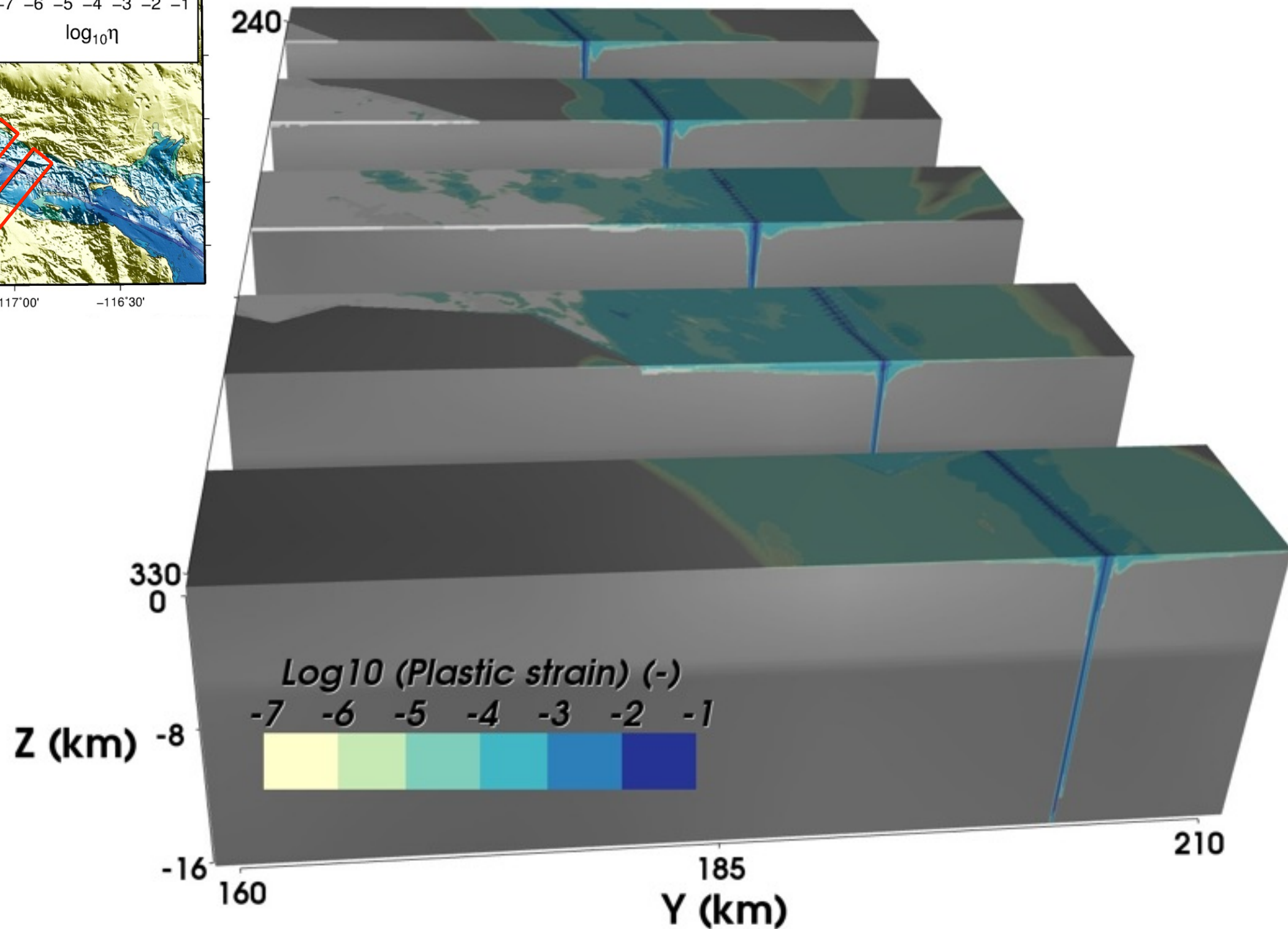
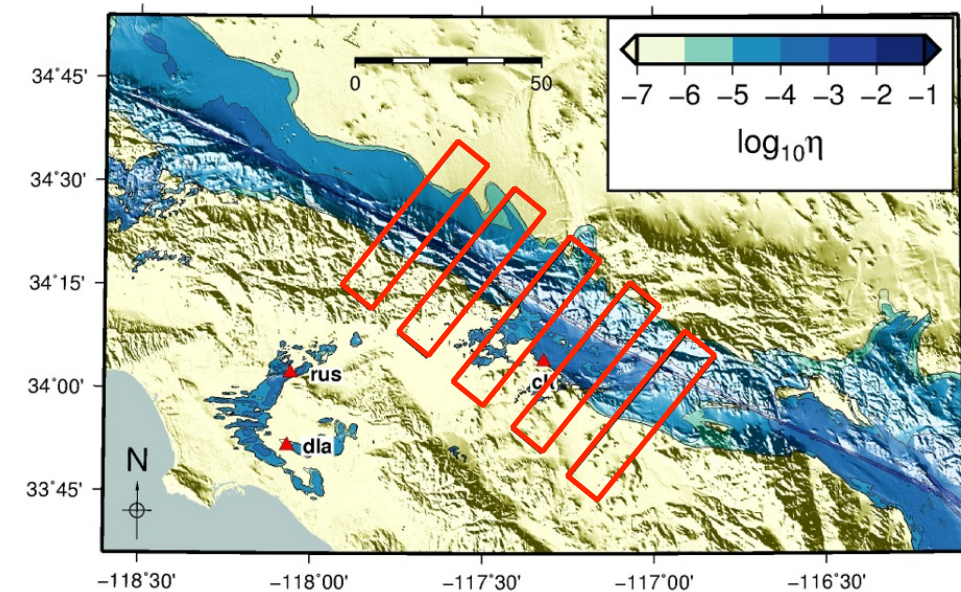
Nonlinear Attenuation of Surface Waves



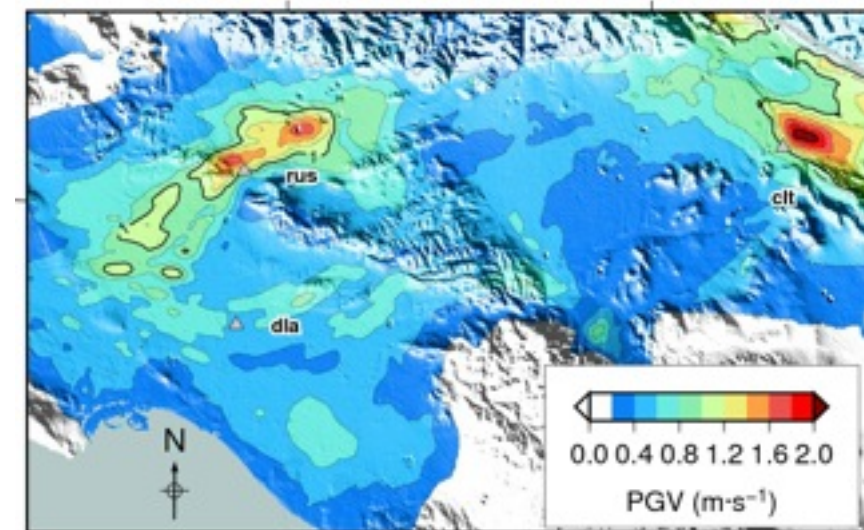
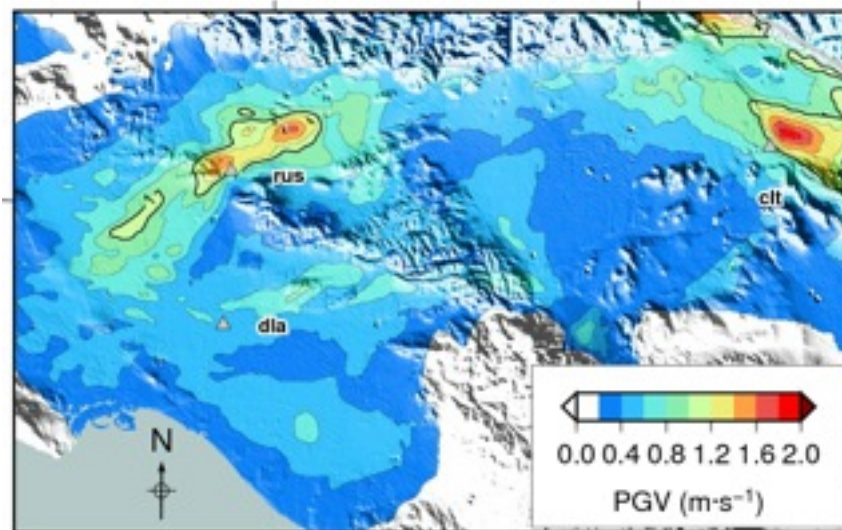
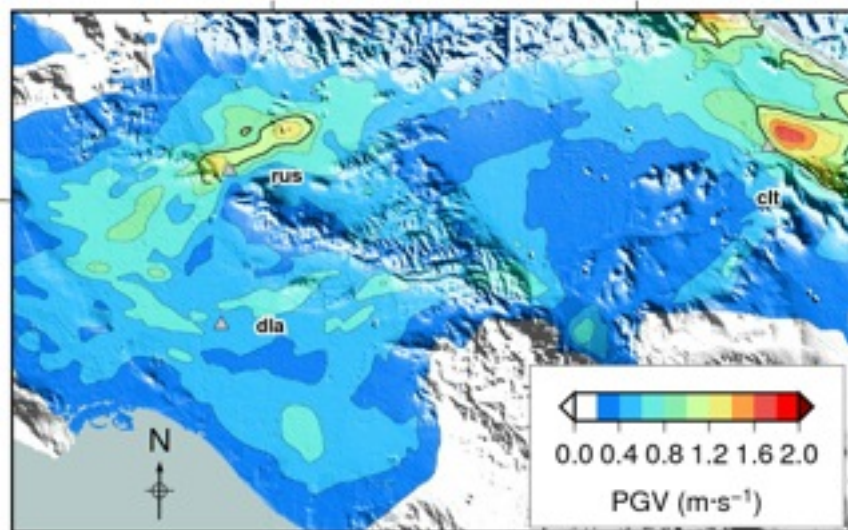
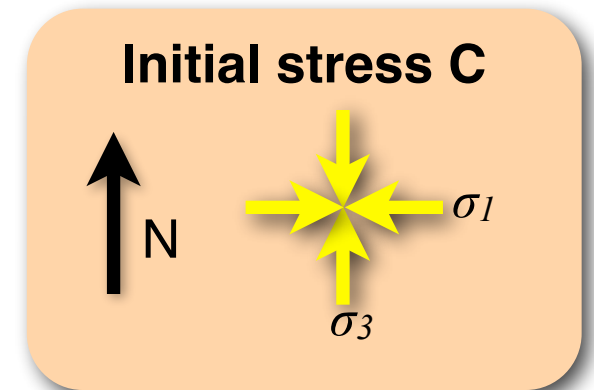
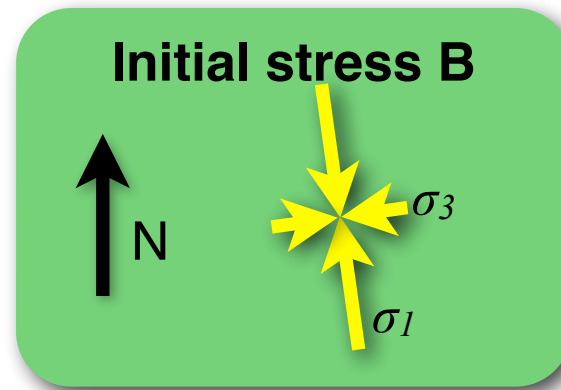
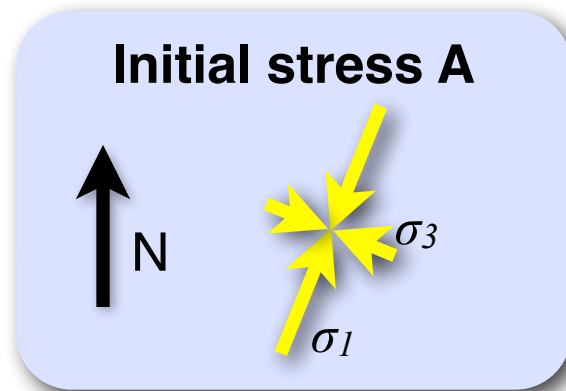
Nonlinear Attenuation of Surface Waves



Nonlinear Attenuation of Surface Waves



Sensitivity to Initial Stress Field



Conclusions

- » We have implemented damage rheology based on the Drucker-Prager yield condition into the highly scalable 3D finite difference code AWP-ODC
- » The method has been verified against independent finite element / finite difference codes in the framework of the SCEC/USGS Spontaneous Rupture Code Verification Project
- » Computational cost of modeling plasticity varies between +10% (GPU version) to +25% (CPU version)
- » We employ the AWP-ODC code to simulate the ShakeOut earthquake scenario for a medium governed by DP-plasticity
- » Nonlinear material behavior could reduce the earlier predictions of large long-period ground motions in the Los Angeles basin (LAB) by 20 - 60% as compared to viscoelastic solutions.
- » These reductions are primarily due to yielding near the fault, although yielding may also occur in the shallow low-velocity deposits of the LAB if cohesions are close to zero.
- » While the amount of reduction is sensitive to the choice of initial stress field and rock strength, the reductions are significant even for conservative estimates.
- » Current simulations assuming a linear response of rocks may overpredict ground motions during future large earthquakes on the southern San Andreas Fault.
- » Future simulations should explore effect of near-surface nonlinearity at higher frequencies

